

May 1981

POR

QUICK LOOK REPORT FOR SEMISCALE

MOD-2A TEST S-UT-6

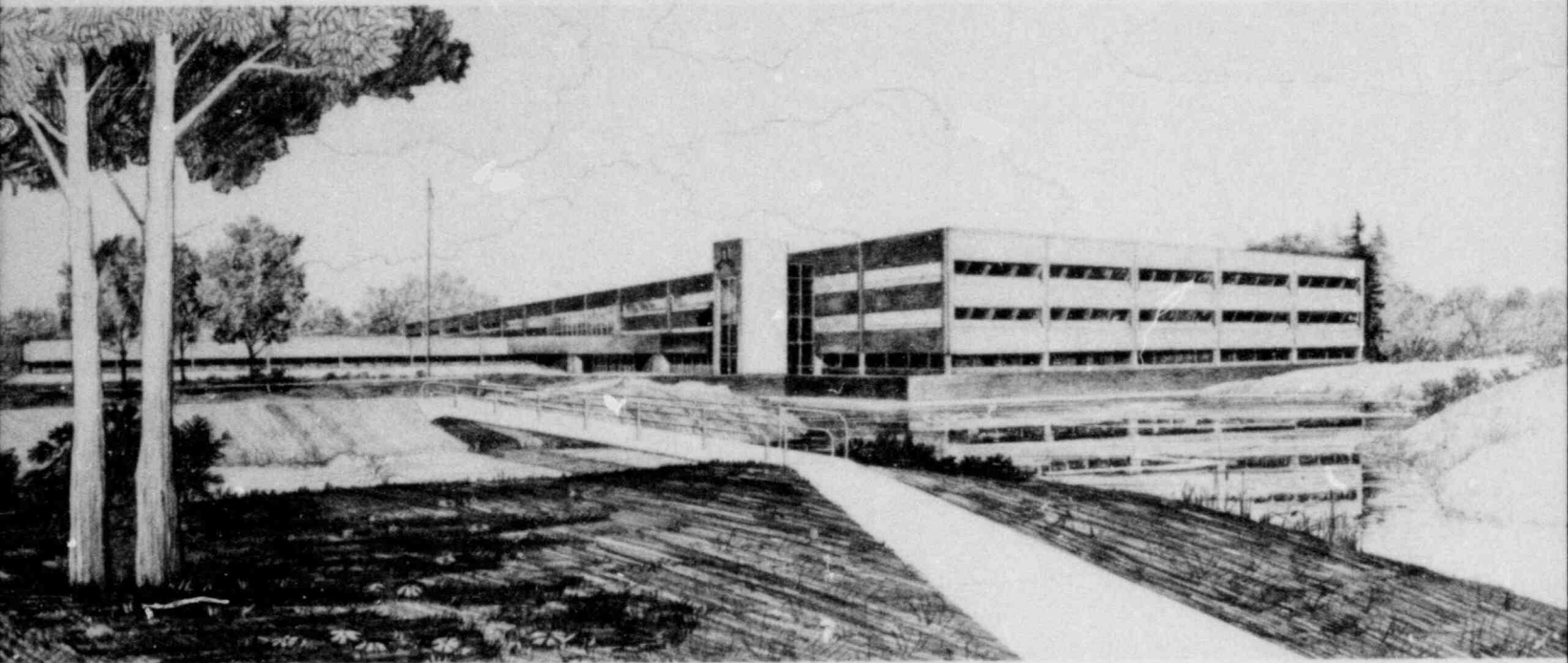
J. M. Cozzuol
C. M. Kullberg

NRC Research and Technical Assistance Report



U.S. Department of Energy

Idaho Operations Office • Idaho National Engineering Laboratory



This is an informal report intended for use as a preliminary or working document

Prepared for the
U.S. Nuclear Regulatory Commission
under DOE Contract No. DE-AC07-761D01570
FIN No. A6038



8107220054 810531
PDR RES
8107220054 PDR

INTERIM REPORT

Accession No. _____

Report No. EGG-SEMI-5446

Contract Program or Project Title:

Water Reactor Research Test Facilities Division

Subject of this Document:

Quick Look Report for Semiscale
Mod-2A Test S-UT-6

Type of Document:

Quick Look Report

Author(s):

J. M. Cozzuol
C. M. Kullberg

Date of Document:

May 13, 1981

**NRC Research and Technical
Assistance Report** ✓

Responsible NRC Individual and NRC Office or Division:

W. C. Lyon, Reactor Safety Research

This document was prepared primarily for preliminary or internal use. It has not received full review and approval. Since there may be substantive changes, this document should not be considered final.

EG&G Idaho, Inc.
Idaho Falls, Idaho 83401

Prepared for the
U.S. Nuclear Regulatory Commission
Washington, D.C.
Under DOE Contract No. **DE-AC07-76ID01570**
NRC FIN No. A6038

INTERIM REPORT

QUICK LOOK REPORT
SEMISCALE MOD-2A
TEST S-UT-6

by

J. M. Cozzuol
C. M. Kullberg

May 1981

Approval: *Gary W. Johnsen*
G. W. Johnsen, Manager
WRRTF Experiment Planning
and Analysis Branch

Approval: *Paul North*
P. North, Manager
Water Reactor Research
Test Facilities Division

ABSTRACT

Results are presented from Semiscale Mod-2A Test S-UT-6. This test was a 5%, communicative, cold leg break loss-of-coolant simulation. The configuration and conditions for the Mod-2A system were equivalent to, or scaled from, a pressurized water reactor equipped with upper head emergency core coolant (ECC) injection capability (UHI). However, no upper head ECC injection was used during the experiment. The test results will provide baseline data on system response to be used for comparison to a 5% break test with UHI (Test S-UT-7).

NRC Research and Technical
Assistance Report

CONTENTS

ABSTRACT	iii
SUMMARY	ix
1. INTRODUCTION	1
2. SYSTEM CONFIGURATION AND TEST CONDUCT	3
2.1 System Configuration	3
2.2 Test Procedures and Conditions	10
2.2.1 Preblowdown Activities	10
2.2.2 Component Controls	11
2.2.3 Initial Conditions and ECC Parameters	15
3. TEST RESULTS	19
3.1 General System Behavior	19
3.2 Pressure Response	19
3.3 Break Response	27
3.4 Loop Hydraulic Response and Void Distribution	31
3.5 Core Response	44
4. COMPARISON OF SELECTED DATA TO PRETEST PREDICTION CALCULATION ...	52
5. CONCLUSIONS	64
APPENDIX A	66

Figures

1.	Semiscale Mod-2A system as configured for Test S-UT-6	4
2.	Communicative break assembly and orifice for 5% break	5
3.	Plan view of the Mod-2A core showing heater rod thermocouple locations for Test S-UT-6	6
4.	Semiscale Mod-2A heater rod axial power distribution	7
5.	Core axial power profile and vessel instrumentation locations	8
6.	Upper head geometry for the Semiscale Mod-2A vessel	9
7.	Core power for Test S-UT-6	12
8.	Intact and broken loop pump speed curves for Test S-UT-6	13
9.	Loop piping heater band power (total) for Test S-UT-6	14
10.	High and low pressure ECC injection system control for intact loop	16
11.	Vessel upper plenum pressure for Test S-UT-6	21
12.	Comparison of fluid temperatures around the system with the saturation temperature	23
13.	Axial density distribution in the core (elevations above bottom of core)	24
14.	Comparison of the break mass flow rate and the HPIS flow rate	25
15.	Comparison of primary and steam generator secondary pressures for Test S-UT-6	26
16.	Break flow rate obtained from condenser catch tank liquid levels	28
17.	Fluid density in the broken loop cold leg on the vessel side of the break orifice	29

18.	Fluid density in the broken loop cold leg on the pump side of the break orifice	30
19.	Collapsed liquid levels in the upflow and downflow sides of the intact loop steam generator	32
20.	Collapsed liquid level in the downflow side of the broken loop steam generator	33
21.	Comparison of upper head fluid temperatures with the saturation temperature (elevations above cold leg centerline)	35
22.	Upper head collapsed liquid level	36
23.	Collapsed liquid levels in the upflow and downflow legs of the intact loop pump suction	37
24.	Collapsed liquid levels in the upflow and downflow legs of the broken loop pump suction	38
25.	Fluid density in the intact loop cold leg near the vessel	40
26.	Volumetric flow in the vessel upper plenum	41
27.	Fluid density in the intact loop hot leg	42
28.	Fluid density in the broken loop hot leg	43
29.	System mass balance using inflow / outflow method and liquid level method	45
30.	Downcomer and core collapsed liquid levels	47
31.	Fluid densities in the core (elevations above bottom of core)	48
32.	Fluid densities in upper half of core illustrating uncovering as a result of boiloff (elevations above bottom of core)	49
33.	Heater rod cladding temperatures illustrating temperature excursion in upper part of core (elevations above bottom of core)	50
34.	Comparison of the calculated and measured system pressure response for Test S-UT-6	54

35.	Comparison of the calculated and measured cold leg temperatures for Test S-UT-6	55
36.	Comparison of the calculated and measured steam generator secondary fluid temperatures and pressures for Test S-UT-6	56
37.	Comparison of the calculated and measured pump suction liquid levels (downflow side) for Test S-UT-6	58
38.	Comparison of the calculated and measured pump suction levels (upflow side) for Test S-UT-6	59
39.	Comparison of calculated and measured upper head and core collapsed liquid levels for Test S-UT-6	60
40.	Comparison of the calculated and measured integrated break mass flow rates for Test S-UT-6	61
41.	Comparison of calculated and measured core heater rod cladding temperature at the midcore region for Test S-UT-6	63
A-1.	Nodalization diagram of the RELAP5 model for the Semiscale Mod-2A system	68

TABLES

1.	Initial Conditions and ECC Requirements for Test S-UT-6	17
2.	Sequence of Events for Test S-UT-6	20
3.	Initial Conditions for Test S-UT-6	53

SUMMARY

This report presents the results of a preliminary analysis of data from Semiscale Mod-2A small break Test S-UT-6. This test simulated a loss-of-coolant accident resulting from 5% communicative break in the cold leg of a pressurized water reactor (PWR). The break size for this test was 0.112 cm^2 which is volumetrically scaled to represent a 15-cm diameter pipe break in a PWR. The Mod-2A system was configured to simulate a PWR with the capability to inject emergency core coolant (ECC) into the vessel upper head. However, for this test, no upper head ECC injection was used. The loop accumulator pressures were set at 2.86 MPa as is nominally specified for upper head injection (UHI) plants. Data from Test S-UT-6 will be used to establish the baseline response of the Mod-2A system for a 5% break. The next test in the UT series (S-UT-7) will be similar to Test S-UT-6 but with upper head ECC injection.

Initial conditions for the test were equivalent to, or scaled from, typical PWR operating conditions. Following rupture of the pressure boundary, continuous depressurization took place and the system was observed to void predominantly from the upper elevations downward. Fluid in the vessel upper head drained from approximately 70 to 210 s. As the system voided, fluid in the pump suction formed a seal which impeded steam flow around the loops. The formation of the pump suction seals had relatively little effect on the liquid level in the core. Once the intact loop pump suction had cleared, the cold leg emptied uncovering the break. A gradual boiloff of the vessel fluid then occurred such that the top of the core became uncovered by about 560 s, resulting in a core temperature excursion. The temperature excursion was of limited significance, however, since the peak cladding temperature of approximately 660 K was less than normal steady-state operating temperatures. The initiation of accumulator flow at approximately 720 s terminated the temperature excursion, and the core was recovered by 1000 s. After accumulator flow ceased (at about 2800 s), refilling of the system was continued throughout the remainder of the test with HPIS flow. The system depressurized to the LPIS setpoint at approximately 4600 s and the test was terminated at 5000 s.

A comparison of the measured data to the pretest code prediction for Test S-UT-6 indicates that the major trends of system thermal-hydraulic response were predicted reasonably well. The code did overpredict a liquid level depression in the core prior to loop seal blowout, however, and also predicted a faster depressurization once the break became uncovered.

1. INTRODUCTION

Testing performed in the Semiscale Mod-2A system is part of the water reactor safety research effort directed toward assessing and improving the analytical capability of computer codes which are used to predict the behavior of pressurized water reactors (PWR's) during postulated accident scenarios. For this purpose, the Mod-2A system was designed as a small-scale model of the primary system of a four loop PWR nuclear generating plant. The system incorporates the major components of a PWR including steam generators, vessel, pumps, pressurizer, and loop piping. One loop (intact loop) is scaled to simulate the three intact loops in a PWR, while the other (broken loop) simulates the single loop in which a break is postulated to occur in a PWR. Geometric similarity has been maintained between a PWR and Mod-2A, most notably in the design of a 25 rod, full-length (3.66 m), electrically heated core, full length upper head and upper plenum, component layout, and relative elevations of various components. Equipment in the upper head of the Mod-2A vessel has been designed to simulate the fluid flow paths found in a PWR which has the capability of injecting emergency core coolant (ECC) into the upper head. The scaling philosophy followed in the design of the Mod-2A system (modified volume scaling) preserves most of the important first order effects thought important for small break loss-of-coolant transients.¹

The current tests being conducted in the Mod-2A system are part of the UT test series. The primary objective of the UT test series is to evaluate the capability of the upper head injection (UHI) system to provide an increased margin against core uncovering in the Semiscale system during small break transients. The test series will investigate transients for 2-1/2%, 5%, and 10% cold leg breaks. For each break size a test is first conducted which does not use UHI but does use loop accumulators pressurized to 2.86 MPa to establish baseline response data. These are followed by similar tests which do employ UHI. Tests results will provide applicable data for use in the assessment of computer codes used to predict the behavior of UHI systems.

This report presents a preliminary analysis of the data from Semiscale Test S-UT-6, the sixth test conducted in the UT test series. Test S-UT-6 was a 5%, communicative, cold leg break loss-of-coolant experiment performed without upper head injection. This test provided data to be used as a baseline for comparison to the next test in the UT series (S-UT-7) which will be a 5% break experiment with ECC injected into the upper head.

The results of the analysis of Test S-UT-6, are discussed in the following sections. Section 2 describes the system hardware, test procedures, and initial conditions. Section 3 presents the results of the test data analysis, Section 4 compares the actual system response with the pretest prediction, and Section 5 presents preliminary conclusions.

2. SYSTEM CONFIGURATION AND TEST CONDUCT

2.1 System Configuration

An isometric of the Semiscale Mod-2A system, as configured for Test S-UT-6, is shown in Figure 1 with major components identified. As shown, a condenser/catch tank system was included to provide an independent measurement of the transient break flow.

The break was located in the broken loop cold leg between the pump and the vessel and was communicative in nature. The break assembly and orifice are shown in detail in Figure 2. The break size was 0.1123 cm^2 , which is volumetrically scaled to represent 5% of the area of a cold leg pipe in a PWR. The orifice was designed as bell-mouthed with a length-to-diameter ratio of 3.

Figure 3 is a plan view of the Mod-2A core for Test S-UT-6 showing its orientation with respect to the remainder of the system, the location of unpowered rods, and the distribution of internal cladding thermocouples monitored during the test. Internally heated electric rods are used to simulate the nuclear rods in a PWR. The rods are geometrically similar to nuclear rods with a heated length of 3.66 m and an outside diameter of 1.072 cm. The axial power profile for the rods is illustrated in Figure 4, showing the step cosine shape with a 1.55 peak to average power factor. All 23 heated rods were powered equally. The total core power was 1.99 MW which yielded a maximum linear heat generation rate of 36.67 kW/m. The relative locations of in-core instrumentation (gamma densitometers and core inlet drag screen) and grid spacers are indicated in Figure 5.

Figure 6 shows the configuration of the upper head region of the Mod-2A vessel. The internals of the upper head have been designed to simulate the flow paths found in a PWR with UHI capability. Penetrations into the upper head consist of a perforated ECC injection tube, (not used in Test S-UT-6), a bypass line from the top of the downcomer, a simulated control rod guide tube, and two simulated support columns.

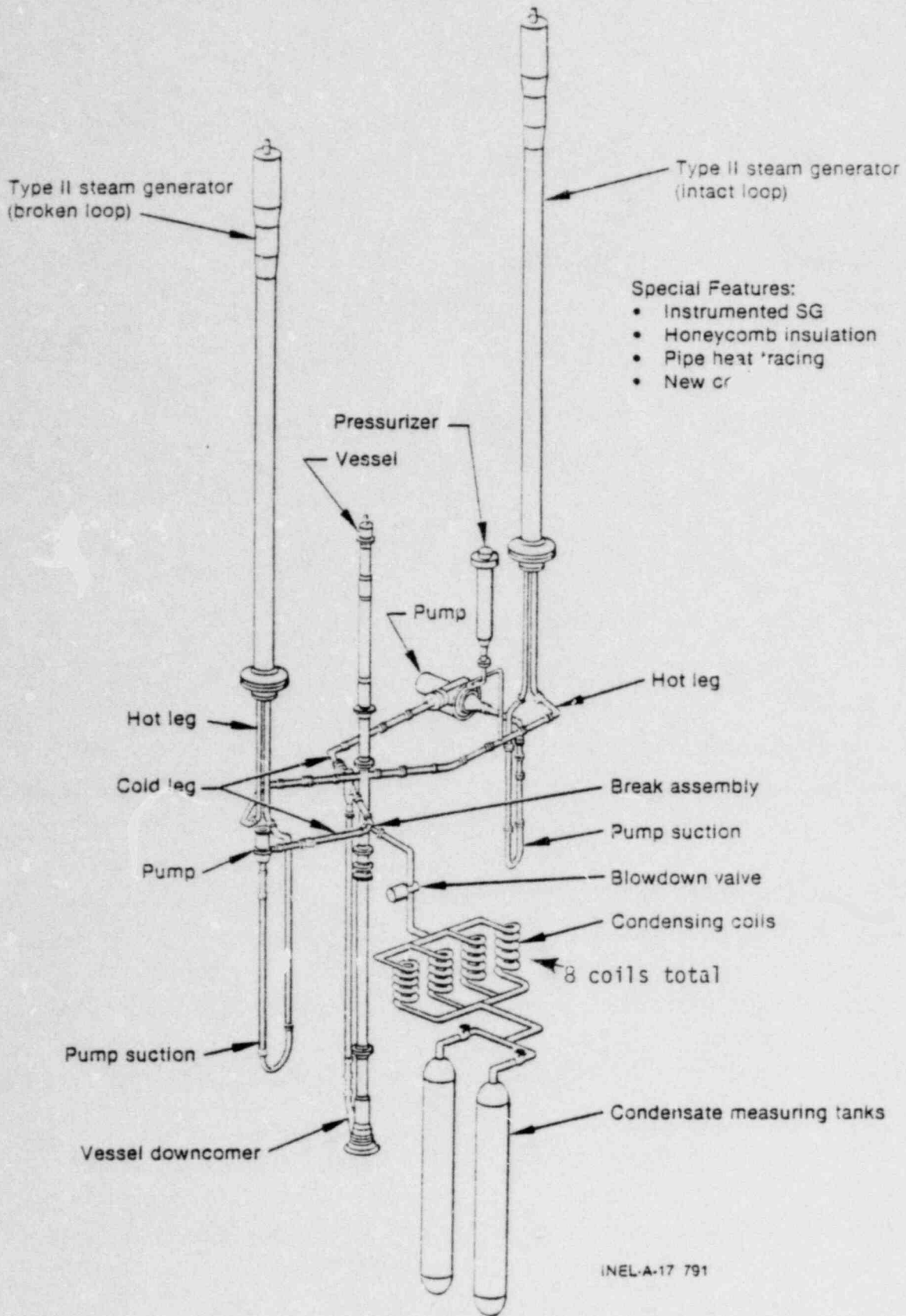
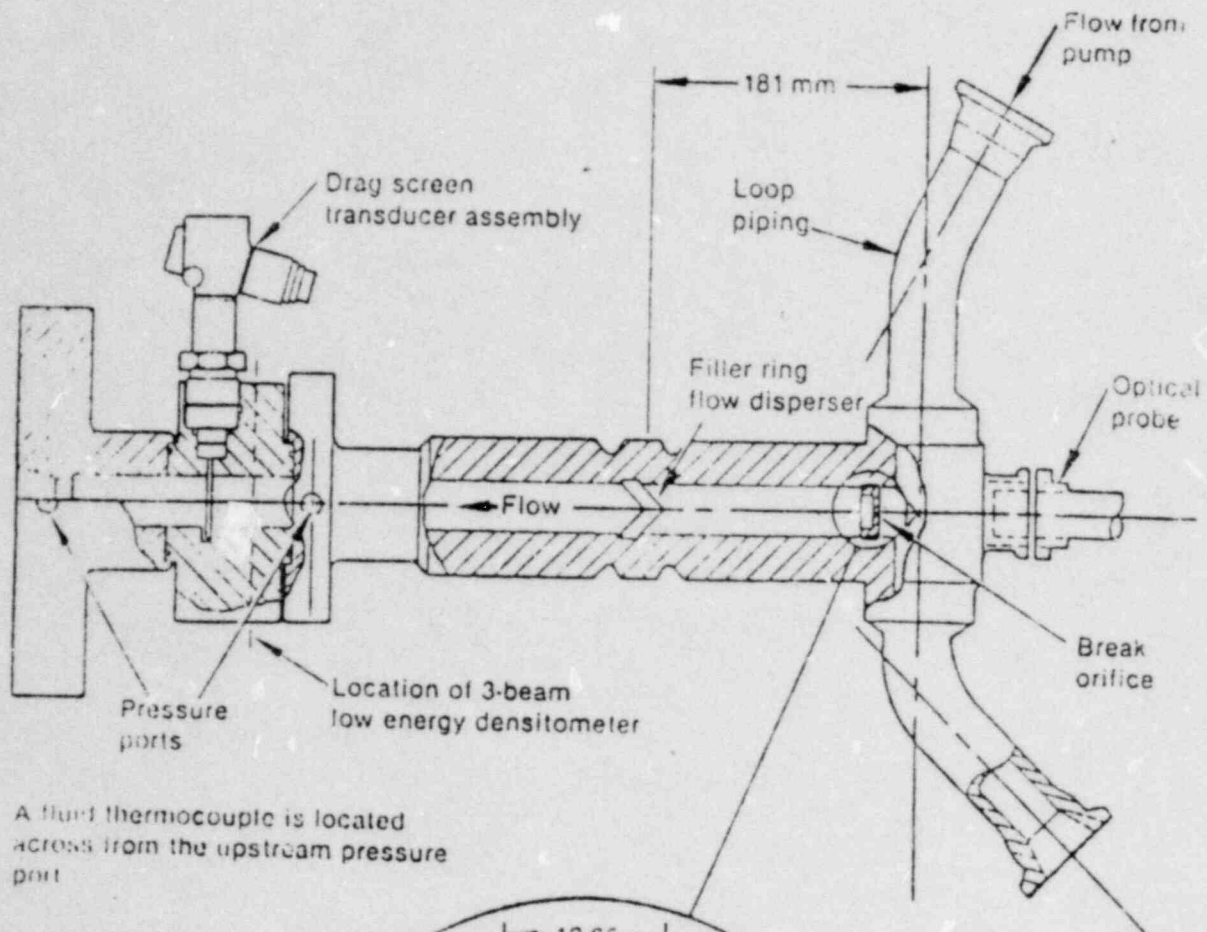
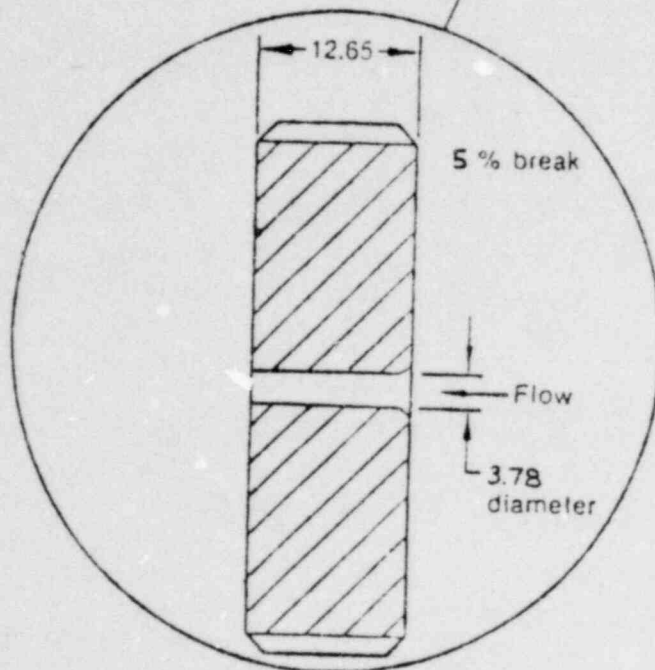


Figure 1. Semiscale Mod-2A system as configured for Test S-UT-6.

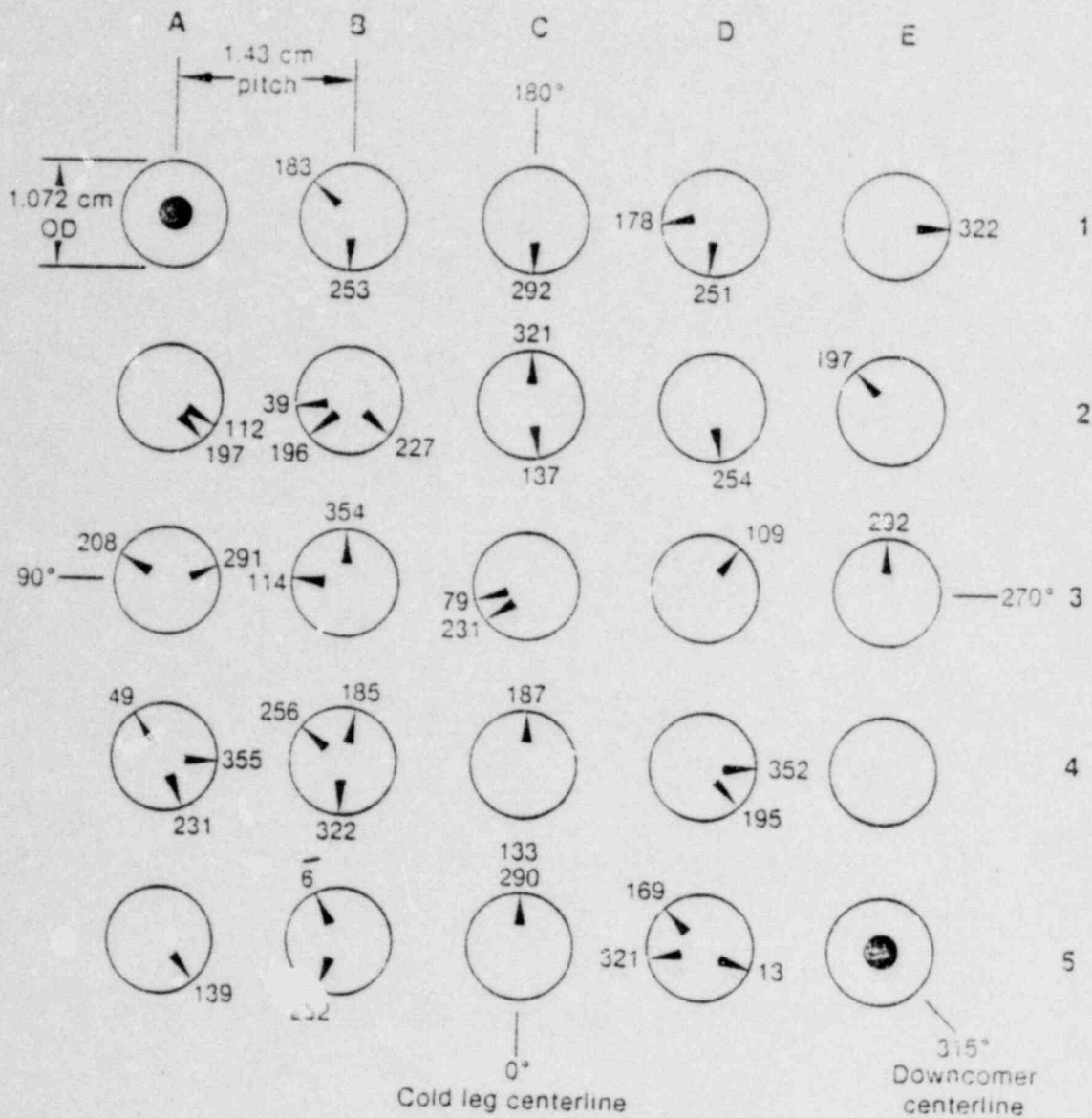


A fluid thermocouple is located across from the upstream pressure port



All dimensions are in mm

Figure 2. Communicative break assembly and orifice for 5% break.



INEL A-17 763

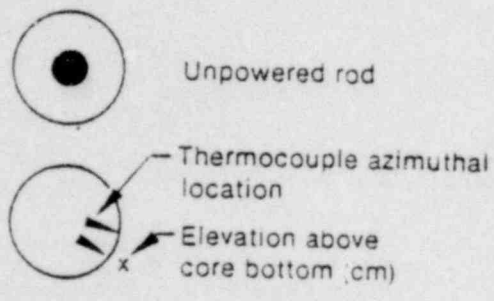


Figure 3. Plan view of the Mod-2A core showing heater rod thermocouple locations for Test S-UT-6.

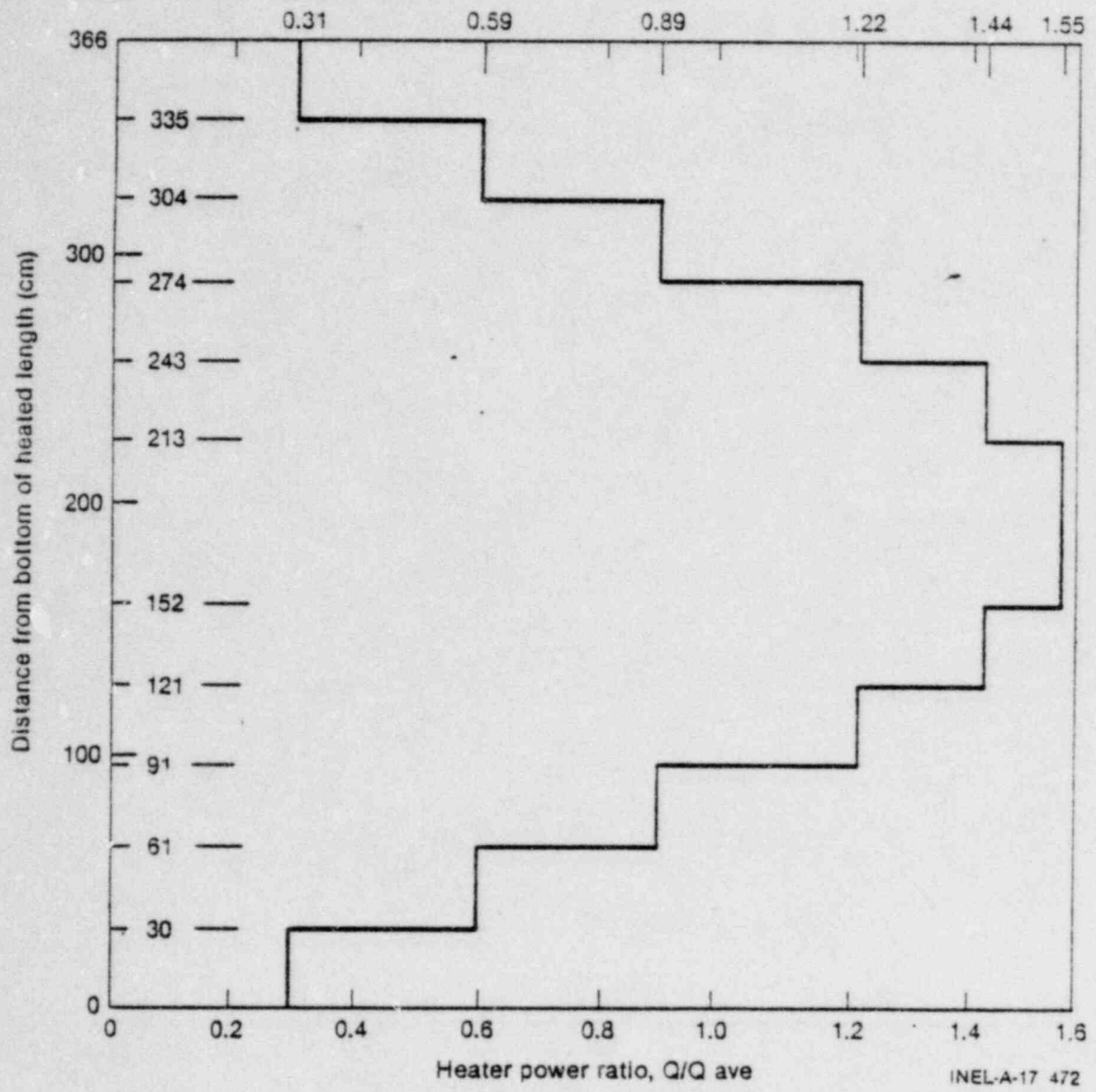


Figure 4. Semiscale Mod-2A heater rod axial power distribution.

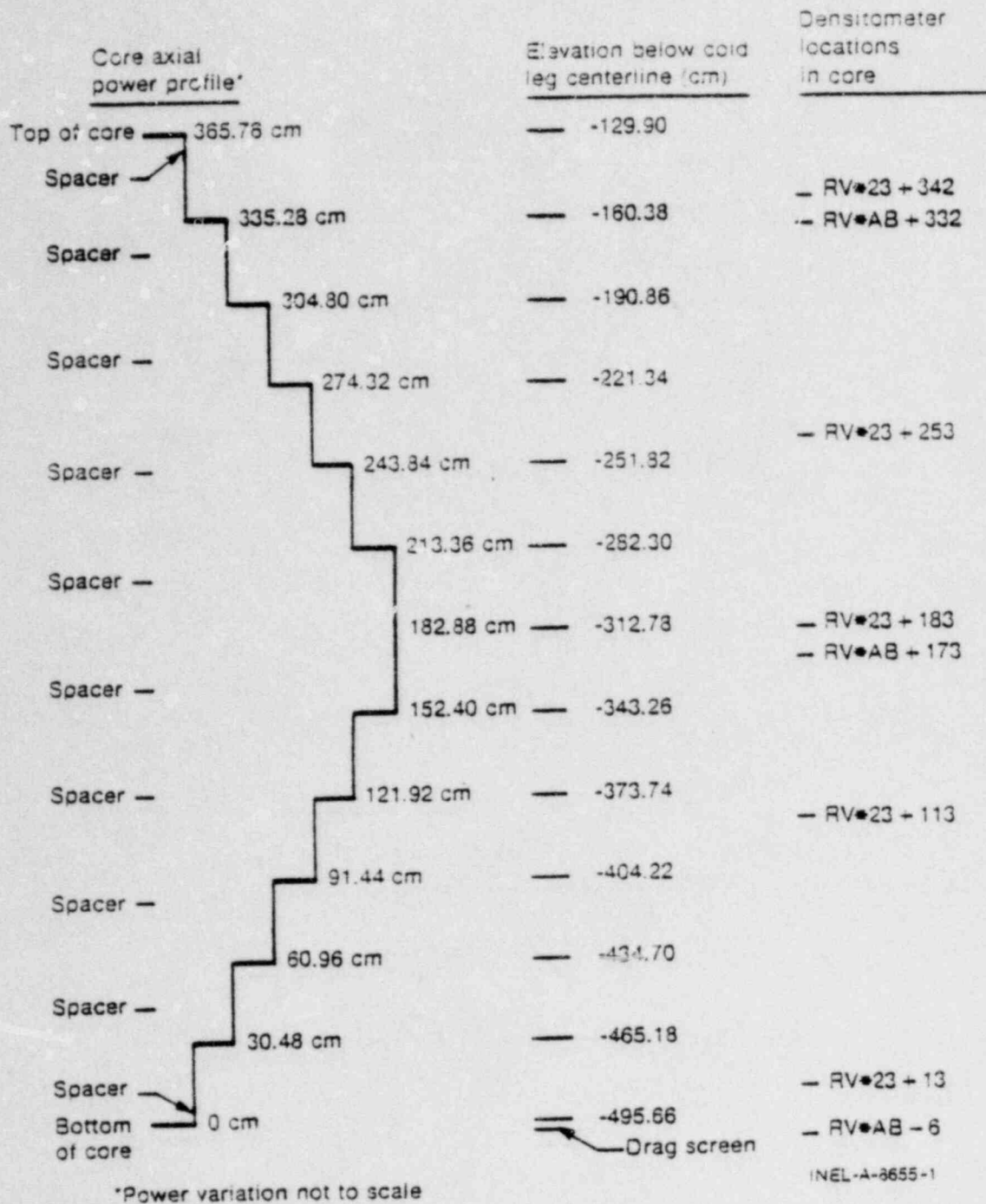


Figure 5. Core axial power profile and vessel instrumentation locations.

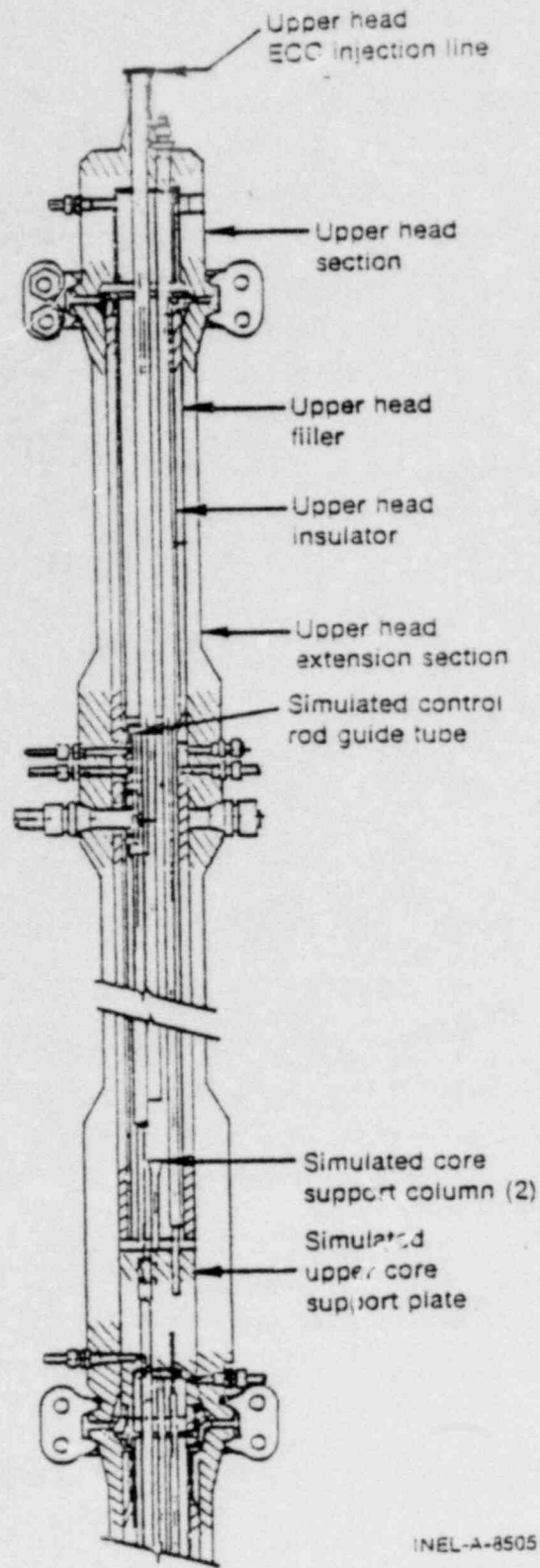


Figure 6. Upper head geometry for the Semiscale Mod-2A vessel.

The heat loss makeup system for the Mod-2A system is composed of numerous heater bands and tapes on the loop piping and five variable power supplies. Heater bands and tape have been installed on the piping where space allows. The heaters are controlled in five power banks; intact loop hot leg, intact loop cold leg, intact loop pump suction, broken loop hot and cold leg, and broken loop pump suction. The total operating capacity of the system is approximately 51 kW. A more detailed description of the system may be found in Reference 2. A representation of the distribution of heaters may be seen in the computer code system model in the appendix.

The data acquisition system recorded measurements from approximately 275 instruments throughout the system. These measurements include fluid and metal temperatures, pressures, fluid densities, flow rates, liquid levels, and other system parameters. Figure 2 shows the communicative break assembly and one set of instrumentation used to measure break flow. A more detailed description of the Mod-2A system may be found in the Semiscale Mod-2A System Design Description.²

2.2 Test Procedures and Conditions

2.2.1 Preblowdown Activities

Prior to the initiation of the test, the Semiscale system was filled with demineralized water and vented to ensure a liquid full system. Water in the steam generator feedwater tank was heated to the desired temperature. Accumulator water levels were established and the accumulators were pressurized with nitrogen gas to the desired pressure. The accumulators used in this test injected water into the intact and broken loop cold legs. Instrumentation was calibrated and zeroed as necessary and a system hydrostatic test was performed.^a After the

a. The measured leak rate for Test S-UT-6 was 0.022 L/s at initial conditions. This is much smaller than the break flow rate during the early portion of the transient. The leak rate generally decreases with system pressure and with increased system voiding.

necessary protective trip controls and peripheral hardware controls (pumps, valves, etc.) had been set, the system was brought to initial conditions and the required levels were established in the steam generator secondary sides. Power for the external heaters on the loops was brought to specified conditions and the system was allowed to equilibrate.

When initial conditions were within specified tolerances, the test was initiated by opening a blowdown valve downstream of the break orifice to break the system pressure boundary.

2.2.2 Component Controls

Transient core power control and the intact and broken loop pump speed controllers were initiated by a pressure trip 3.4 s after the pressurizer pressure reached 12.8 MPa. Both intact and broken loop steam generator steam valves were sequenced to close when the pressurizer pressure reached 12.6 MPa. Both steam generator feedwater valves were sequenced to close 24 s after the pressurizer pressure reached 12.6 MPa.^a The core power curve and pump speed curves are shown in Figures 7 and 8 respectively. More discussion of how the core electric power curve was determined, and how other various component controls were selected, may be found in Reference 3.

The heaters on the intact and broken loop piping were controlled to offset system heat losses to the extent possible. The power to the heaters was determined by analysis of pretest scoping calculations which compared Mod-2A response for various control schemes against an ideal system with no heat losses. Heater band power was controlled on-line according to the data presented in Figure 9. The heaters are initially powered at 51 kW which is approximately the maximum system operating limit. Power was decreased as the transient proceeded in response to the predicted voiding of the loops and resultant decreased fluid to pipe heat transfer.

a. The Mod-2A steam generators operate with a lower than desired secondary liquid level at initial conditions. Extra feedwater is injected for 24 s to ensure that the tubes are covered for the transient.

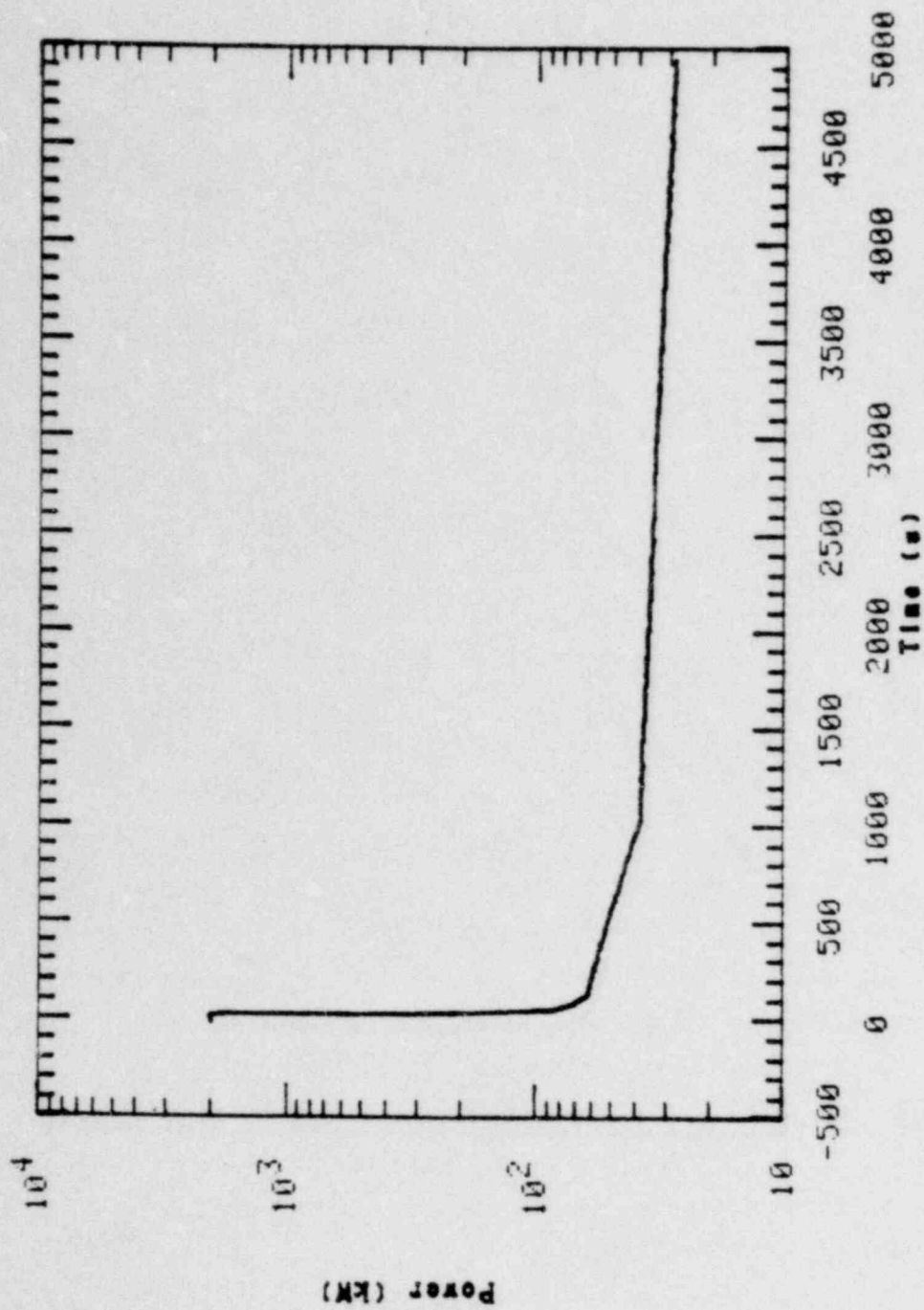


Figure 7. Core power for Test S-IJT-6.

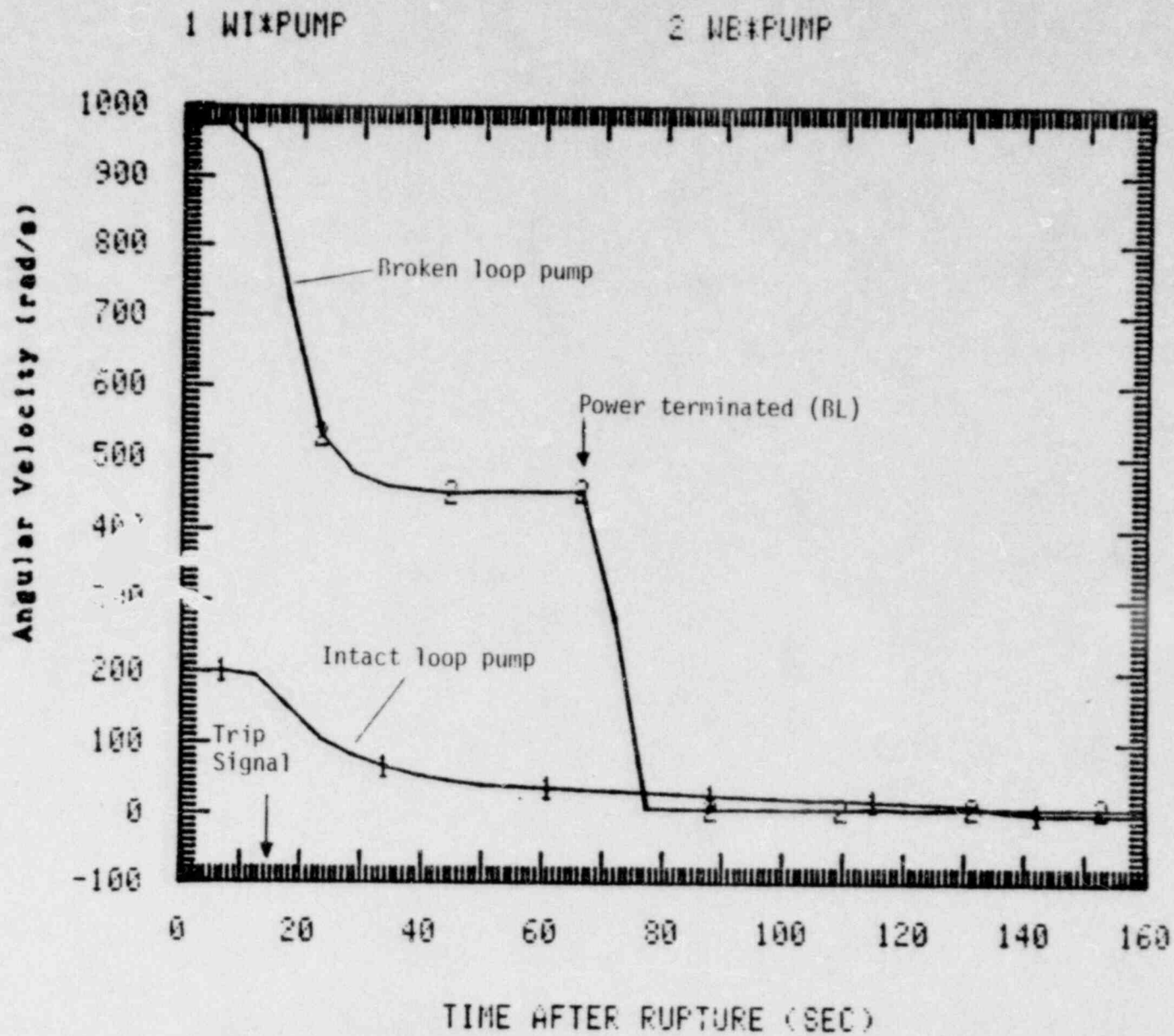


Figure 8. Intact and broken loop pump speed curves for Test S-UT-6.

1 HEATER BAND PGWE

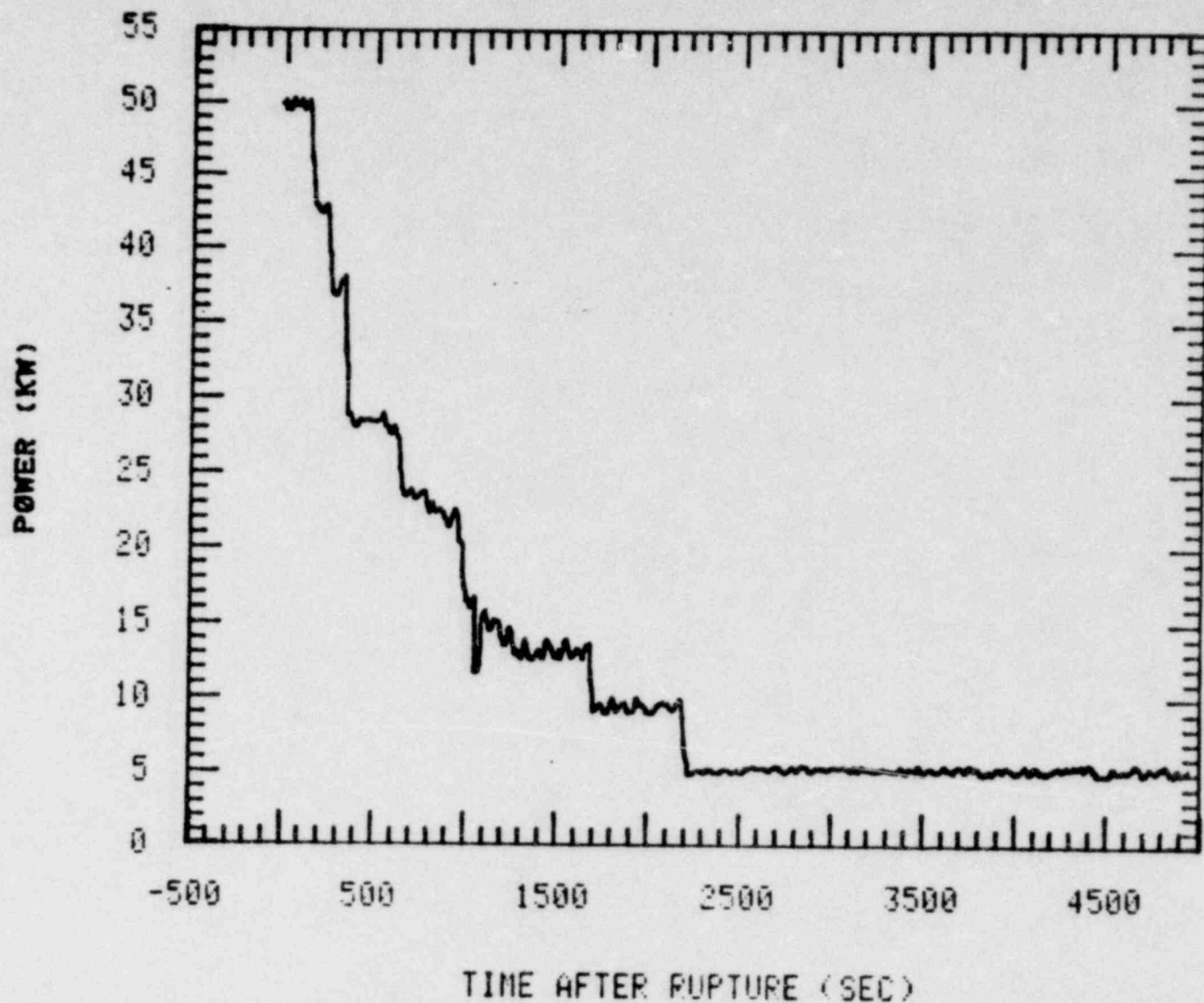


Figure 9. Loop piping heater band power (total) for Test S-UT-6.

The HPIS and LPIS flow rates were controlled on a flow rate versus system pressure basis to simulate the characteristics of a PWR plant with one train each of HPIS and LPIS in operation. A three-to-one flow split between the intact and broken loop injection rates was specified for the test. However, the broken loop HPIS/LPIS pump was mistakenly not operated. The flow rate versus pressure curve used to control the intact loop HPIS and LPIS flow rate is shown in Figure 10. Since a single pump is used in each loop to simulate the HPI and LPI systems, the LPIS injection rate is simply added to the HPIS flow rate for pressure below 0.98 MPa.

2.2.3 Initial Conditions and ECC Parameters

The specified and actual test conditions for Test S-UT-6 are compared in Table 1. In general, the initial conditions and test parameters were judged satisfactory to meet the test objectives. One notable difference between the actual and specified ECC parameters was the lack of ECC injection into the broken loop, resulting in only about 75% of the specified HPIS/LPIS fluid being injected into the system (intact loop cold leg) during the transient. However, based on previous small break experiments, it is evident that much of the broken loop HPIS liquid exits the system via the break before it can get to the vessel. It is thus concluded that the lack of broken loop HPIS did not significantly affect the amount of liquid available in the vessel/core, and thus did not influence the core thermal-hydraulic response during the transient.

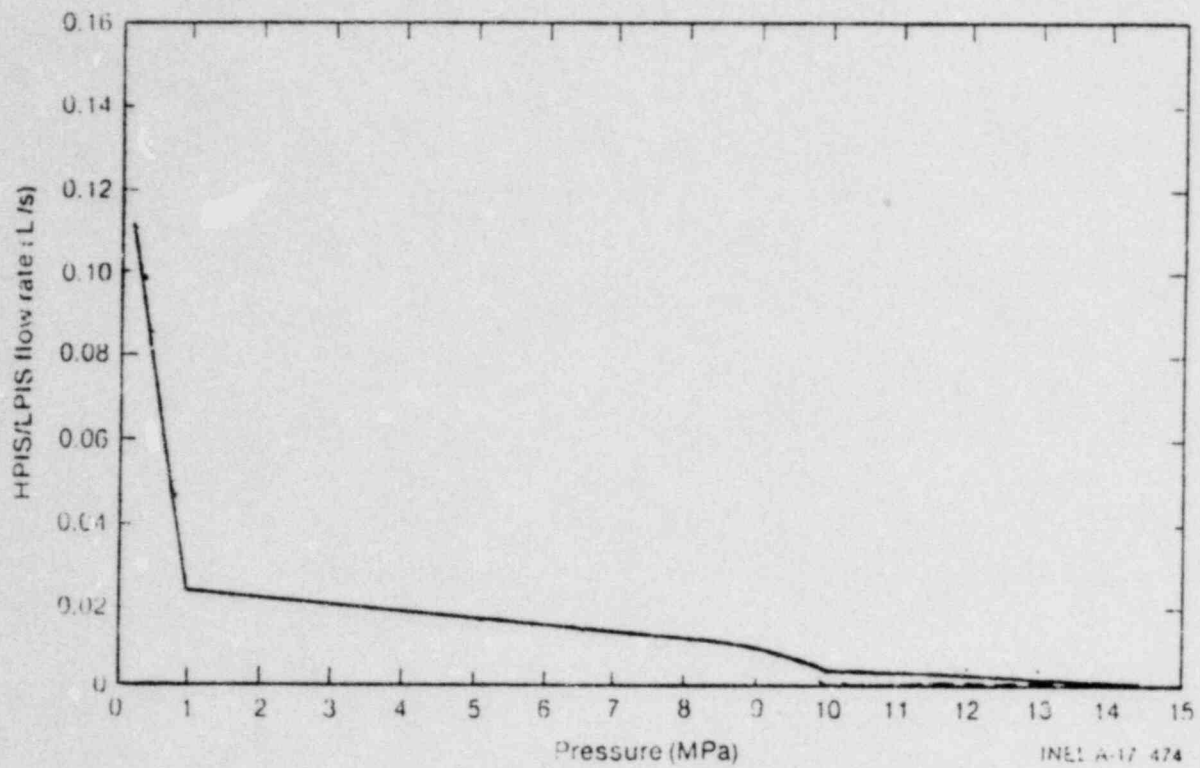


Figure 10. High and low pressure ECC injection system control for intact loop.

TABLE 1. INITIAL CONDITIONS AND ECC REQUIREMENTS FOR TEST S-UT-6

Parameter	Specified Value	Actual Value
<u>Initial Conditions</u>		
System pressure	15.5 ± 0.2 MPa	15.6 MPa
Hot leg fluid temperature	594 ± 2 K	597 K
Cold leg fluid temperature	557 ± 2 K	557 K
Total core power	2.0 ± 0.005 MW	1.99 MW
Radial power profile	Flat	
Core inlet flow rate	9.77 kg/s ^a	9.1 kg/s
Pressurizer liquid mass	10.4 ± 0.1 kg	10.3 kg ^d
S.G. secondary pressure	5.9 ± 0.2 MPa ^d	Intact loop 5.7 MPa Broken loop 5.9 MPa
S.G. feedwater temperature	495 ± 2 K	Intact loop 504 K Broken loop 504 K
S.G. steam dome temperature	547 ± 2 K ^d	Intact loop 545 K Broken loop 546 K
S.G. secondary water level		
Intact loop	Footnote b	1037 cm ^e
Broken loop	Footnote b	809 cm ^e
<u>Configuration</u>		
Break size	5%	
Break type	Communicative	
Break location	Cold leg	
Pressurizer location	Intact loop	
Pressurizer line resistance	5.9 x 10 ⁸ m ⁻⁴ d	
<u>ECC Injection</u>		
Intact loop accumulator		
Actuation pressure	2.9 ± 0.1 MPa	2.8 MPa _a
Liquid volume	0.048 ± 0.0005 m ³	0.045 m ³
Nitrogen volume	0.025 ± 0.0005 m ³	0.027 m ³
Temperature	300 ± 10 K	300 K
Line resistance	8.59 x 10 ⁸ m ⁻⁴ d	
Intact loop HPIS		
Actuation pressure	12.6 ± 0.1 MPa	12.6 MPa
Delay	25 ± 0.5 s	25 s
Injection rate	See Figure 10 ^c	
Temperature	300 ± 10 K	300 K
Intact loop LPIS		
Actuation pressure	0.98 MPa ± 0.05 MPa	0.98 MPa
Injection rate	See Figure 10	
Temperature	300 ± 10 K	300 K

TABLE 1. (continued)

Parameter	Specified Value	Actual Value
Broken loop accumulator		
Actuation pressure	2.9 ± 0.1 MPa	2.8 MPa
Liquid volume	0.016 ± 0.0005 m ³	0.013 m ³
Nitrogen volume	0.0083 ± 0.0005 m ³	0.010 m ³
Temperature	300 ± 10 K	300 K
Line resistance	7.73×10^9 m ⁻⁴ d	
Broken loop HPIS	Not operated	Not operated
Broken loop LPIS	Not operated	Not operated

-
- a. Approximate value; flow is adjusted to achieve required core ΔT .
- b. Secondary side conditions will be adjusted to obtain required primary side temperature and ΔT .
- c. Figure 10 shows the sum of the scaled flow rates for charging and safety injection pumps.
- d. These values are determined by pretest calibrations or through use of process instrumentation.
- e. The reported level is the height of hot water above the top of the tube sheets after the feedwater flow had stopped (24 s after the pressurizer pressure reached 12.6 MPa). The intact loop feedwater flow averaged 1.84 kg/s and the broken loop feedwater flow averaged 0.30 kg/s.
-

3. TEST RESULTS

The following sections present the results of the preliminary analysis of data from Test S-UT-6. First, a brief overview of the general system response is given. This is followed by a more detailed analysis of the more significant aspects of the system behavior, including a discussion of the pressure response, break flow, loop hydraulics and void distribution, and the core thermal-hydraulic behavior.

3.1 General System Behavior

A sequence of events highlighting the important operational and thermal-hydraulic events of Test S-UT-6 is presented in Table 2. The system response was characterized by a continuous depressurization, with voiding occurring from the upper elevations downward early in the transient, followed by a gradual increase in the primary system mass inventory once accumulator injection began. The formation of liquid seals in the pump suction legs (referred to as loop seals) during the early part of the transient had little effect on the vessel liquid level, and no uncovering of the core was observed during this period. After the intact loop seal blew out (at approximately 220 s), a slow boiloff of fluid in the vessel occurred such that the core began to uncover by approximately 560 s causing a core temperature excursion. The vessel/downcomer liquid inventory continued to decrease, reaching a minimum just prior to initiation of accumulator injection at about 730 s. The peak cladding temperature observed during this period was about 660 K and occurred just above the core high power zone. Once accumulator injection began, the core temperature transient was terminated and a gradual filling of the vessel occurred.

3.2 Pressure Response

Figure 11 shows the upper plenum pressure response for Test S-UT-6, and indicates the timing of events which represent major influences on the system depressurization rate. Initially, the system depressurized rapidly

TABLE 2. SEQUENCE OF EVENTS FOR TEST S-UT-6

Event	Time (s)
Blowdown initiated	0
Upper plenum fluid saturates	9.5
Pressurizer pressure = 12.8 MPa	10.3
Intact and broken loop main steam valves begin to close	10.3
Core power decay initiated	12.6
Intact and broken loop pump coastdown initiated	14.3
Pressurizer and surge line empty	28
Entire system saturated	30 to 35
Intact and broken loop main feed-water valves begin to close	34
HPIS initiated	35.2
Power to broken loop pump terminated	67
Power to intact loop pump terminated	134
Upper head drained	210
Intact loop pump suction downflow leg clears out and break uncovers	220
Core begins to uncover	560
Intact loop accumulator injection begins	730
Broken loop accumulator injection begins	750
Core recovered	1000
Broken loop accumulator empties	1250
Intact loop accumulator empties	2800
LPIS setpoint pressure reached	4600
Test terminated	5000

1 PV#UP-13

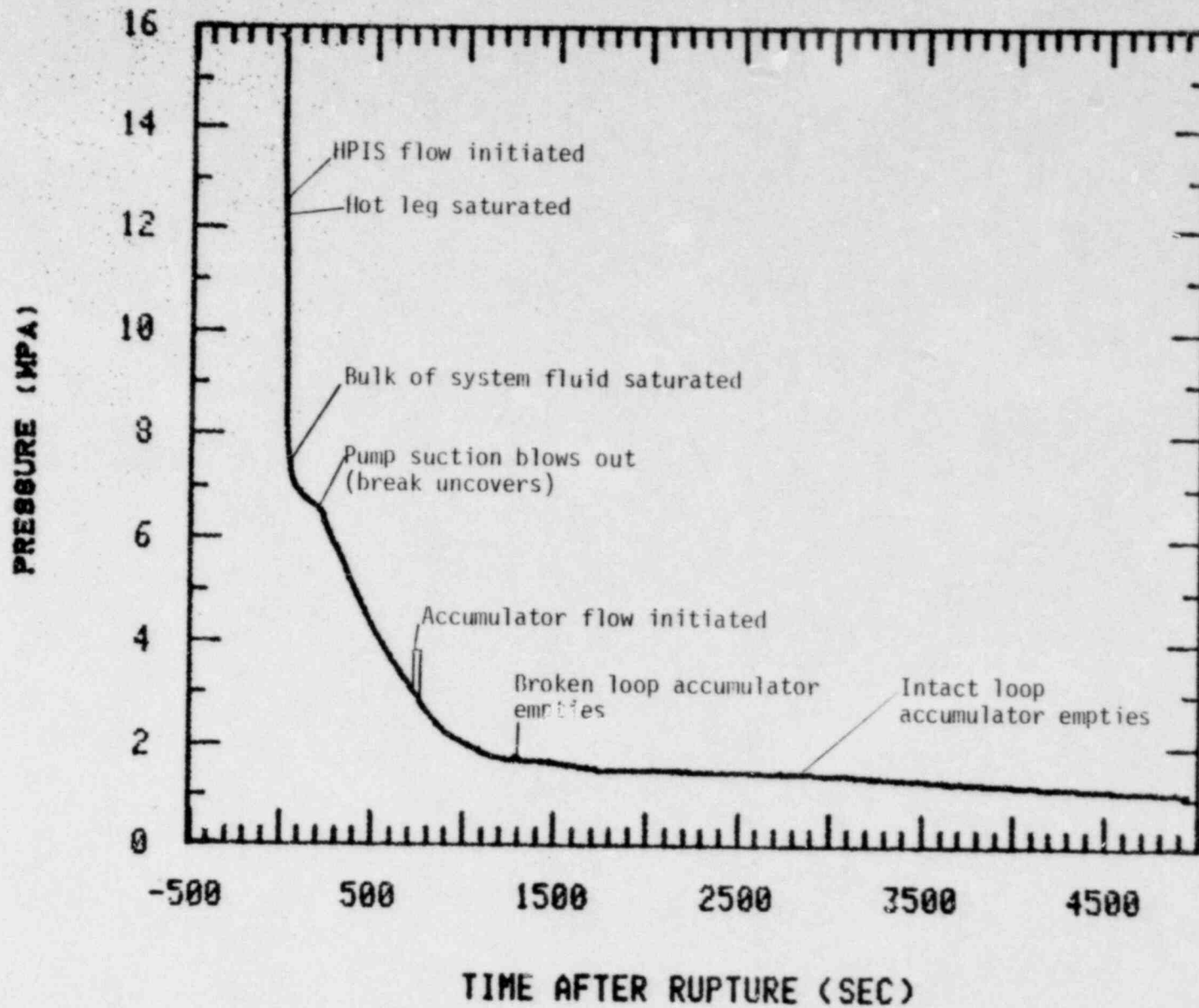


Figure 11. Vessel upper plenum pressure for Test S-UT-6.

to the saturation pressure of the bulk of the system fluid Figure 12, which compares fluid temperatures around the system with the saturation temperature, shows that most of the system fluid became saturated by about 30 s at a temperature somewhat above the initial cold leg temperature. Even though significant flashing of fluid in the cold legs, downcomer, and lower plenum region was not evident at this time, the increased rate of boiling which occurred in the core region and hot legs was sufficient to slow the rate of depressurization causing the knee in the pressure curve shown in Figure 11. The additional steam generation in the core region at this time is indicated in Figure 13 by the decrease in fluid density from all liquid to two-phase values at several elevations in the core.

At about 220 s, the depressurization rate increased somewhat as blowout of the liquid in the intact loop pump suction leg occurred. The blowout of the loop seal at this time caused the break orifice to become uncovered allowing steam flow out the break. The resulting higher energy break flow (high quality steam) in turn caused the more rapid depressurization of the system shown in Figure 11.

The initiation of accumulator injection at about 730 s (2.86 MPa system pressure) again slowed the rate of system depressurization. The partial refilling of the core with accumulator liquid led to an increase in the steam generation rate and a corresponding reduction in the system depressurization rate. By the time the accumulator had emptied (at about 2800 s), the break flow rate was of the same order as the HPIS flow rate (as indicated in Figure 14), and only a minor increase in the rate of depressurization was observed. The pressure continued to decrease at a gradual rate (10 kPa/min) until the LPIS setpoint pressure was reached at about 4600 s. The test was terminated at 5000 s.

As has been observed in previous small break experiments in the Mod-2A system, the influence of the steam generators on the primary system pressure response was negligible once liquid drained from the primary tubes. Figure 15 compares the primary and secondary side pressures and

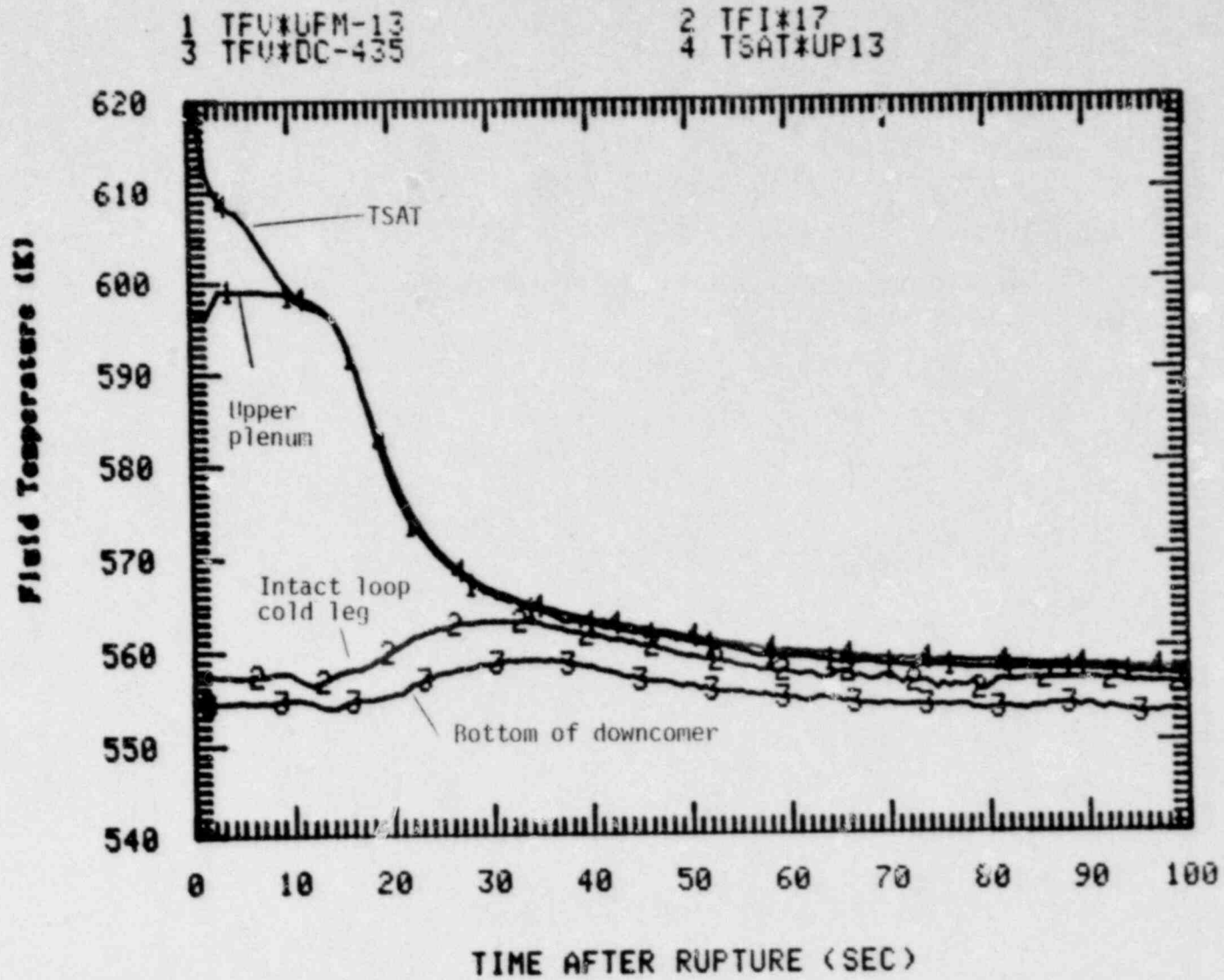


Figure 12. Comparison of fluid temperatures around the system with the saturation temperature.

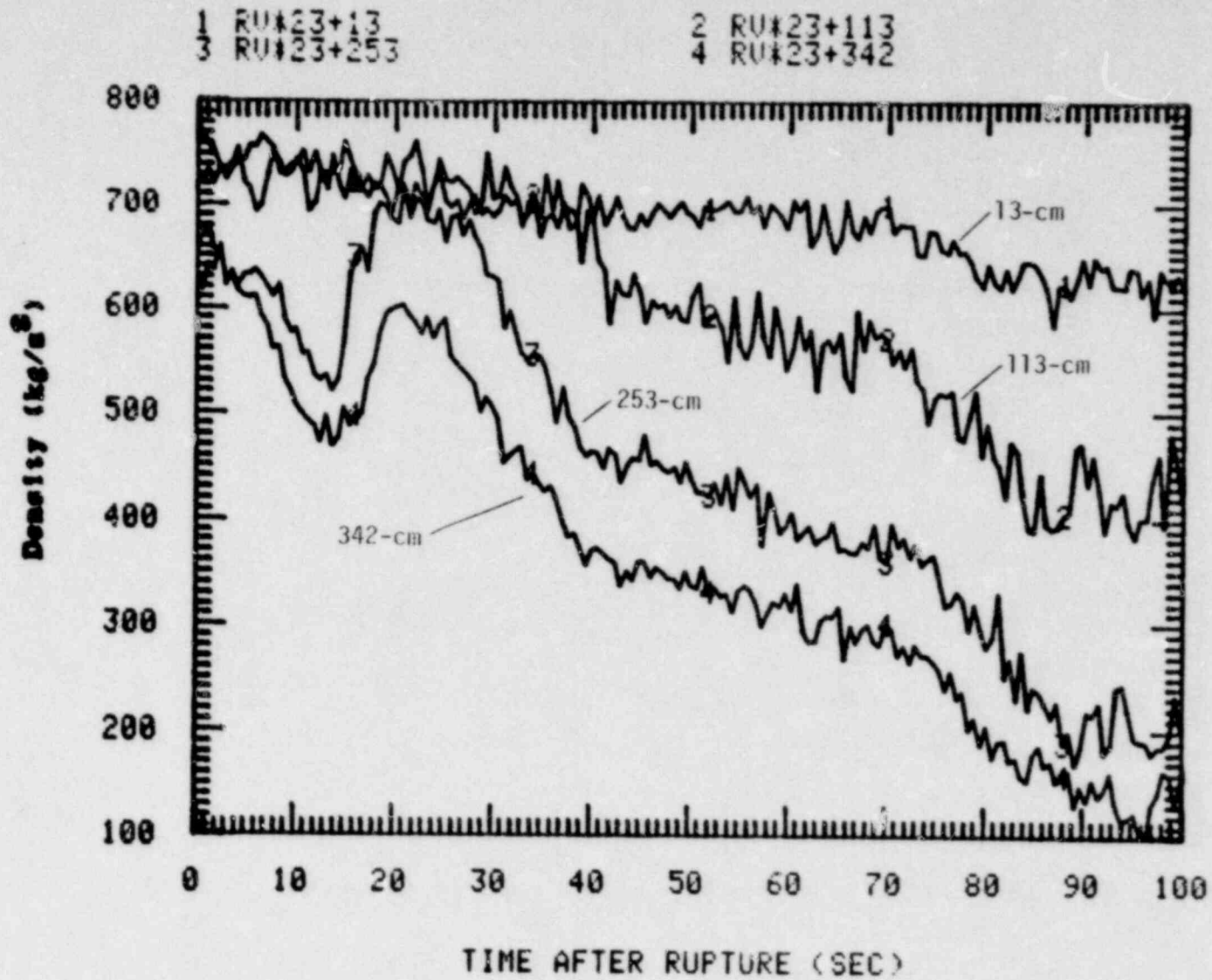


Figure 13. Axial density distribution in the core (elevations above bottom of core).

1 MDCT441(6)*

2 ILHP+LPIS

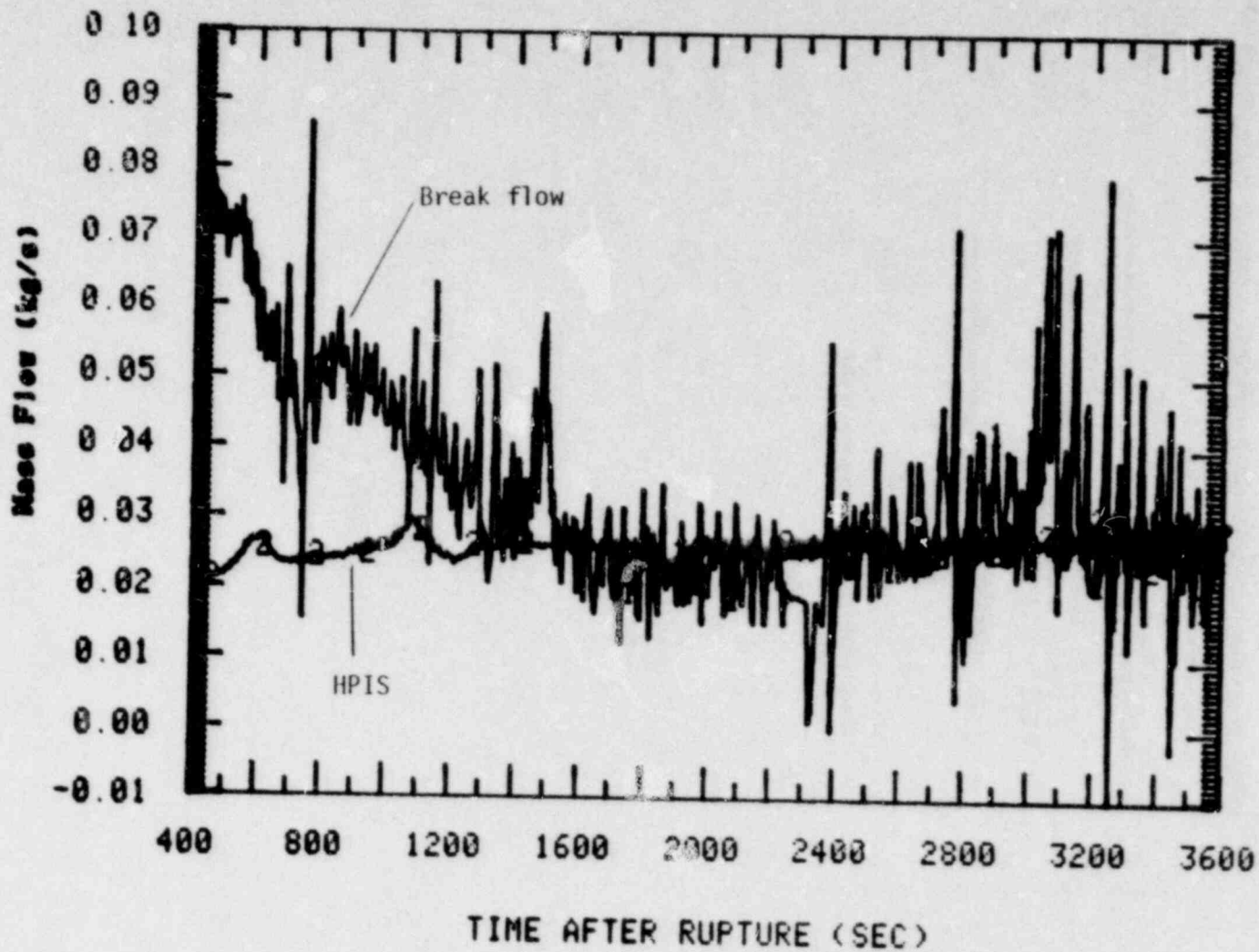


Figure 14. Comparison of the break mass flow rate and the HPIS flow rate.

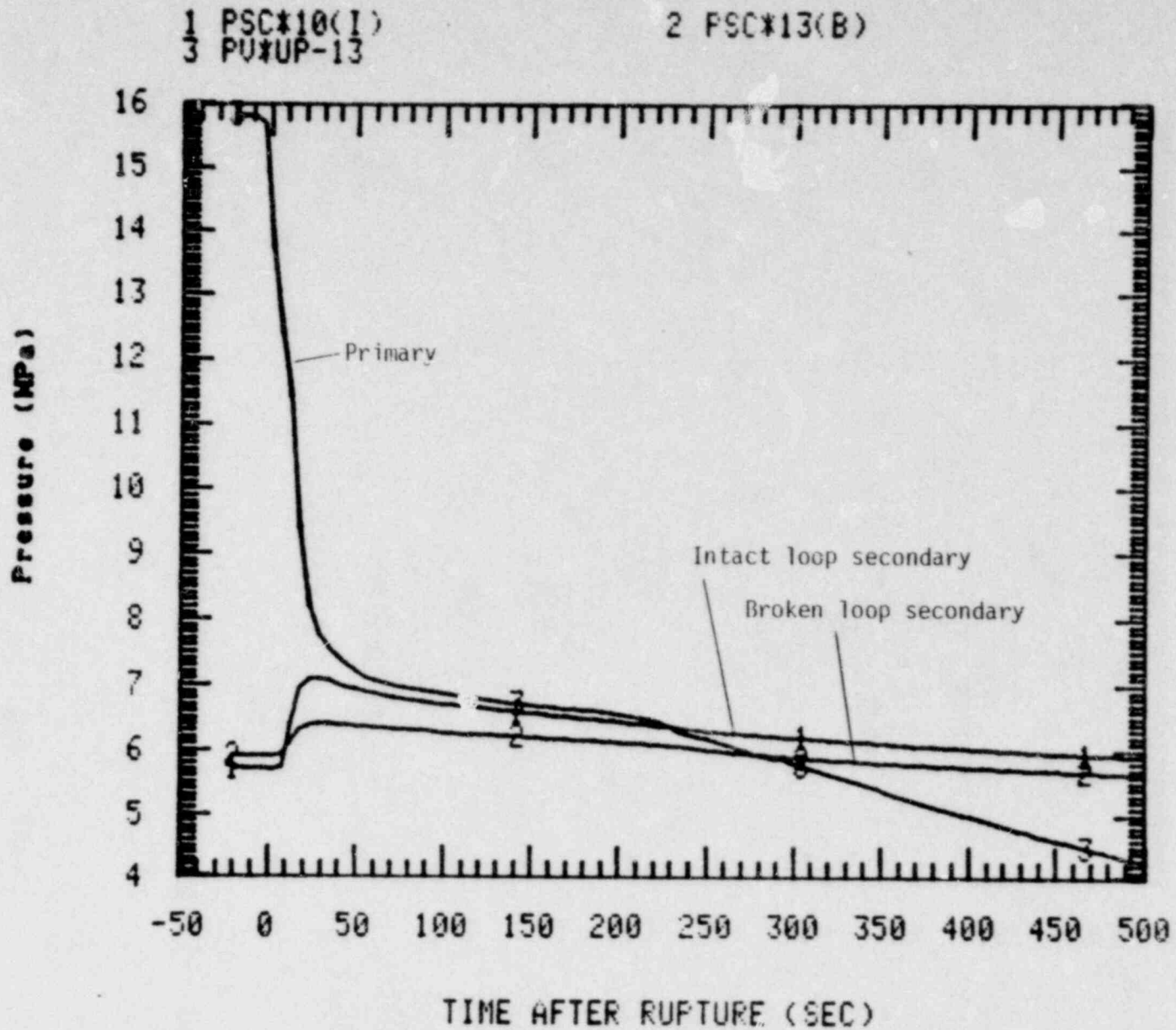


Figure 15. Comparison of primary and steam generator secondary pressures for Test S-UT-6.

indicates that the intact and broken loop steam generators became heat sources at about 230 and 280 s, respectively. However, the relatively slow and small change in secondary side pressures throughout the transient indicate that the primary and secondary sides were essentially decoupled for most of the transient. This can be attributed to the fact that the primary tubes were drained early in the transient, and heat transfer from the secondary fluid to steam in the primary side was minimal.

3.3 Break Response

As indicated previously, a break flow condensing and catch tank system was incorporated in the Mod-2A system for Test S-UT-6 to provide a measurement of the break flow response. Figure 16 shows the break mass flow rate as calculated from the differential pressure (liquid level) measurements in each of the condenser catch tanks. While a lag time for the condenser/catch tank system of 5 to 10 s was apparent based on the relatively slow rise time of the initial flow surge, the measurement is considered to be quite good for the remainder of the transient. The break flow was characterized by a large flow spike early in the transient as the system depressurized to the saturation pressure of the bulk of the system fluid, followed by a period of relatively high flow (until about 230 s) during which saturated liquid was present at the break location, and finally followed by a period of greatly reduced mass flow once the break became uncovered. Figures 17 and 18 show the fluid densities in the primary system spool pieces on either side of the break orifice. The densities show that the primary piping in the break region remained predominantly full until the intact loop pump suction blew out (at about 220 s). At this time the fluid density on the vessel side of the break location (Figure 17) decreased rapidly to a single-phase steam value, indicating that the fluid density at the inlet to the break orifice changed from a two-phase mixture to high quality steam. Although the fluid density measurement on the pump side of the break location (Figure 18) shows that a layer of liquid remained in the bottom of the pipe after the intact loop pump seal blowout occurred, visual observation of the break orifice (using

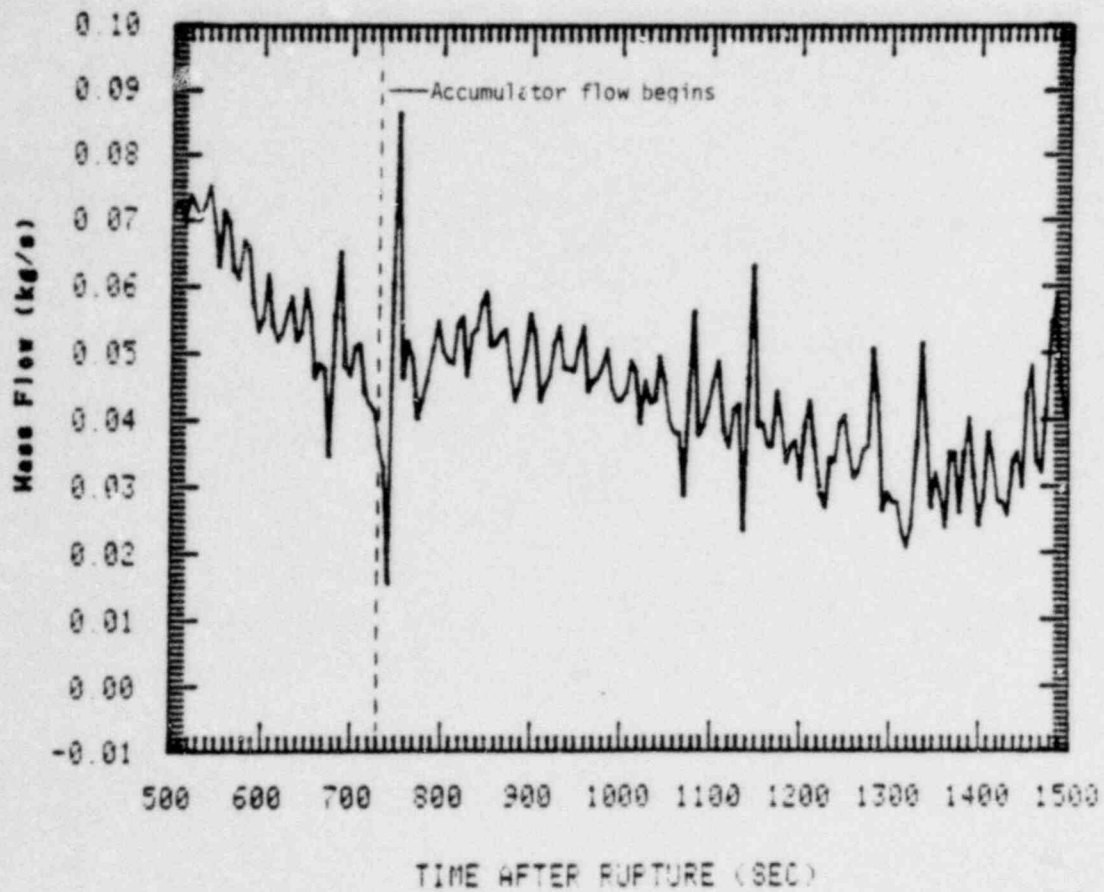
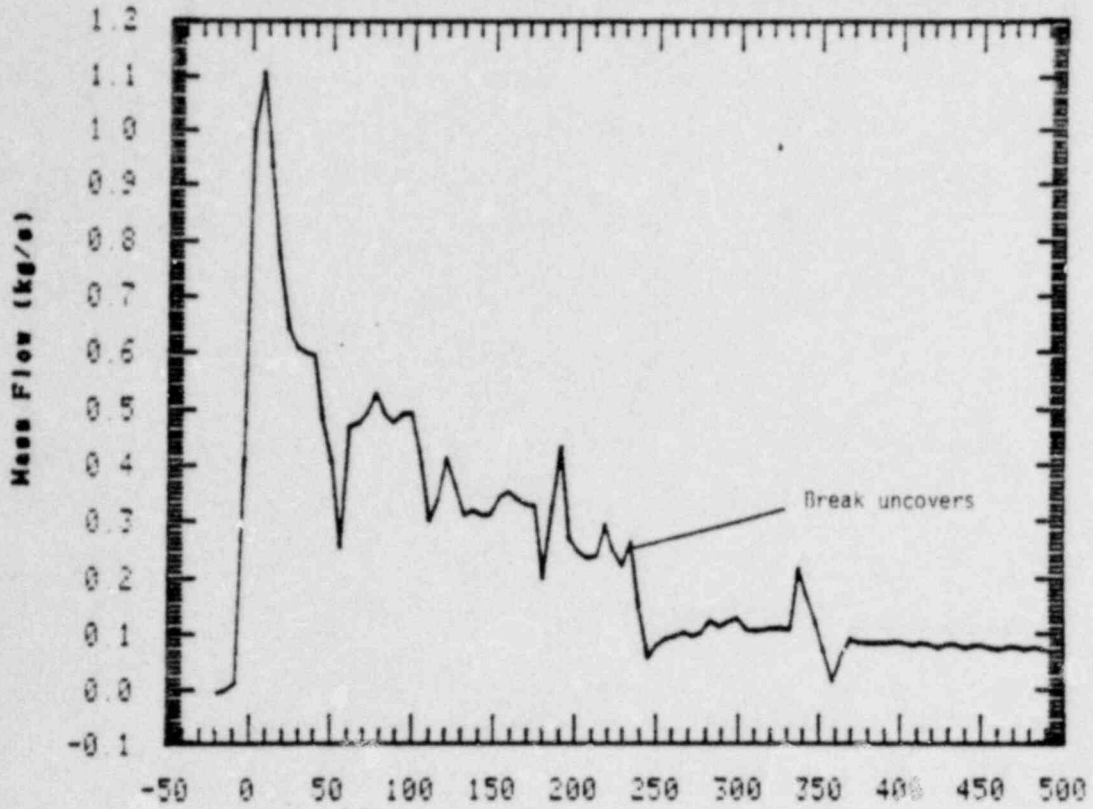


Figure 16. Break flow rate obtained from condenser catch tank liquid levels.

1 RB45B

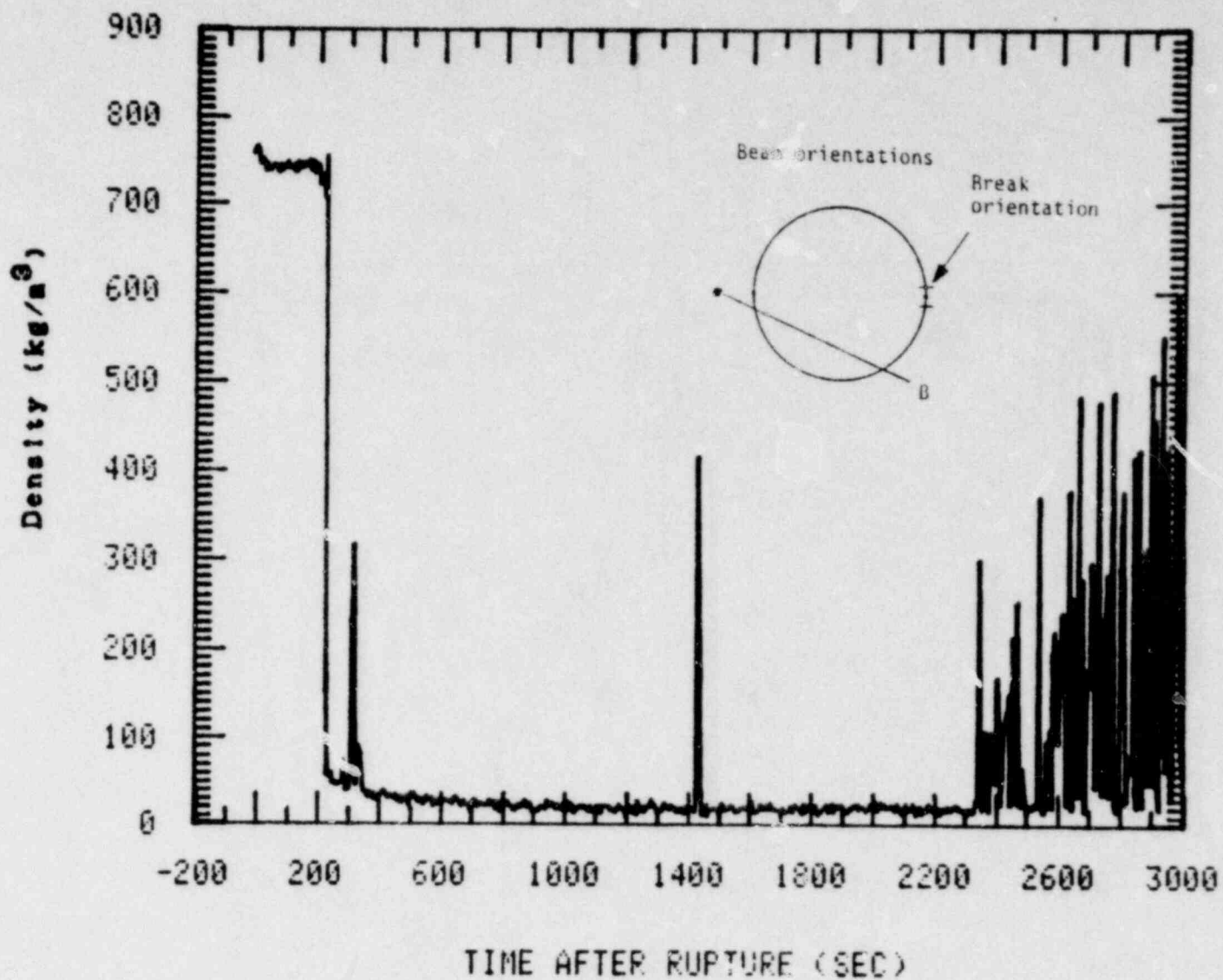


Figure 17. Fluid density in the broken loop cold leg on the vessel side of the break orifice.

1 RB*40M

2 PB*40B

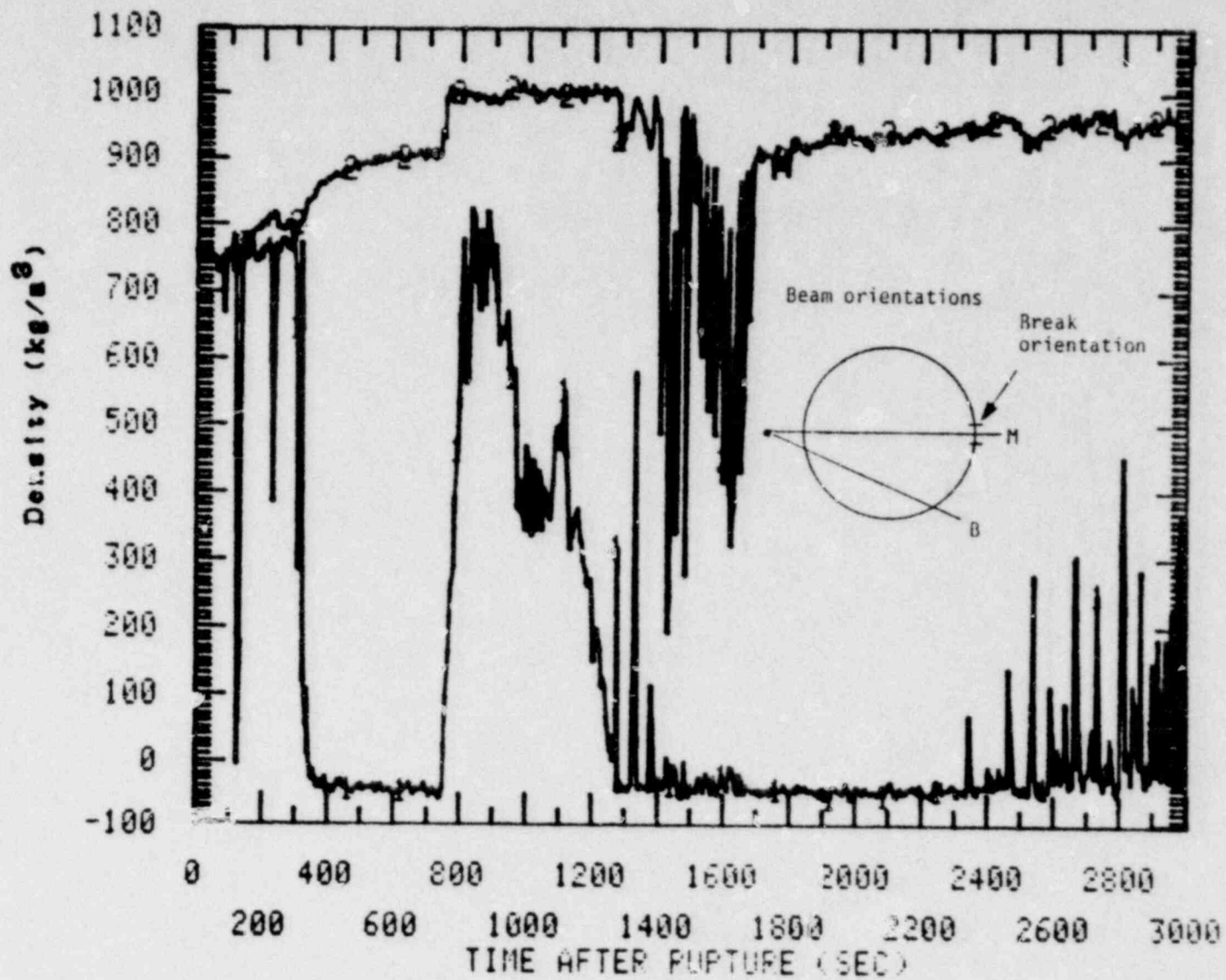


Figure 18. Fluid density in the broken loop cold leg on the pump side of the break orifice.

an optical probe) indicates that the break did become completely uncovered. The resulting decrease in break flow at this time is evident in Figure 16.

The steam flow out the break continued until accumulator injection began at about 750 s. While the accumulators were injecting, a small increase in the break flow rate was observed (Figure 16) indicating that accumulator liquid was leaving the system through the break. Comparing the densities in the spool pieces on either side of the break location (Figures 17 and 18), it is evident that most of the broken loop accumulator fluid exited the system through the break, since the density measurement in the primary piping on the vessel side of the break is indicative of a steam environment during the injection period (750 to 1250 s for the broken loop accumulator). These figures also indicate, however, that there was essentially no bypass of the intact loop accumulator liquid to the broken loop. Thus, all of the intact loop accumulator liquid was available for core cooling.

3.4 Loop Hydraulic Response and Void Distribution

The system behavior during the first 250 s of the transient was characterized by voiding in the upper elevations of the system with liquid collecting in the lower elevations. Fluid in the upper plenum and upper part of the core became saturated by about 8 s, and the steam formed in these regions flowed into the hot legs and steam generators. The continued flow of steam into the steam generators caused liquid to drain out both sides of the inverted U-tubes into the hot legs and pump suction, respectively. Figure 19 compares the collapsed liquid levels in the upflow and downflow sides of the intact loop steam generator, and Figure 20 shows the liquid level on the downflow side of the broken loop steam generator. The data indicate that both the upflow and downflow sides of the intact loop steam generator and the downflow side of the broken loop steam generator were drained by between 120 to 140 s, although steam flow in the

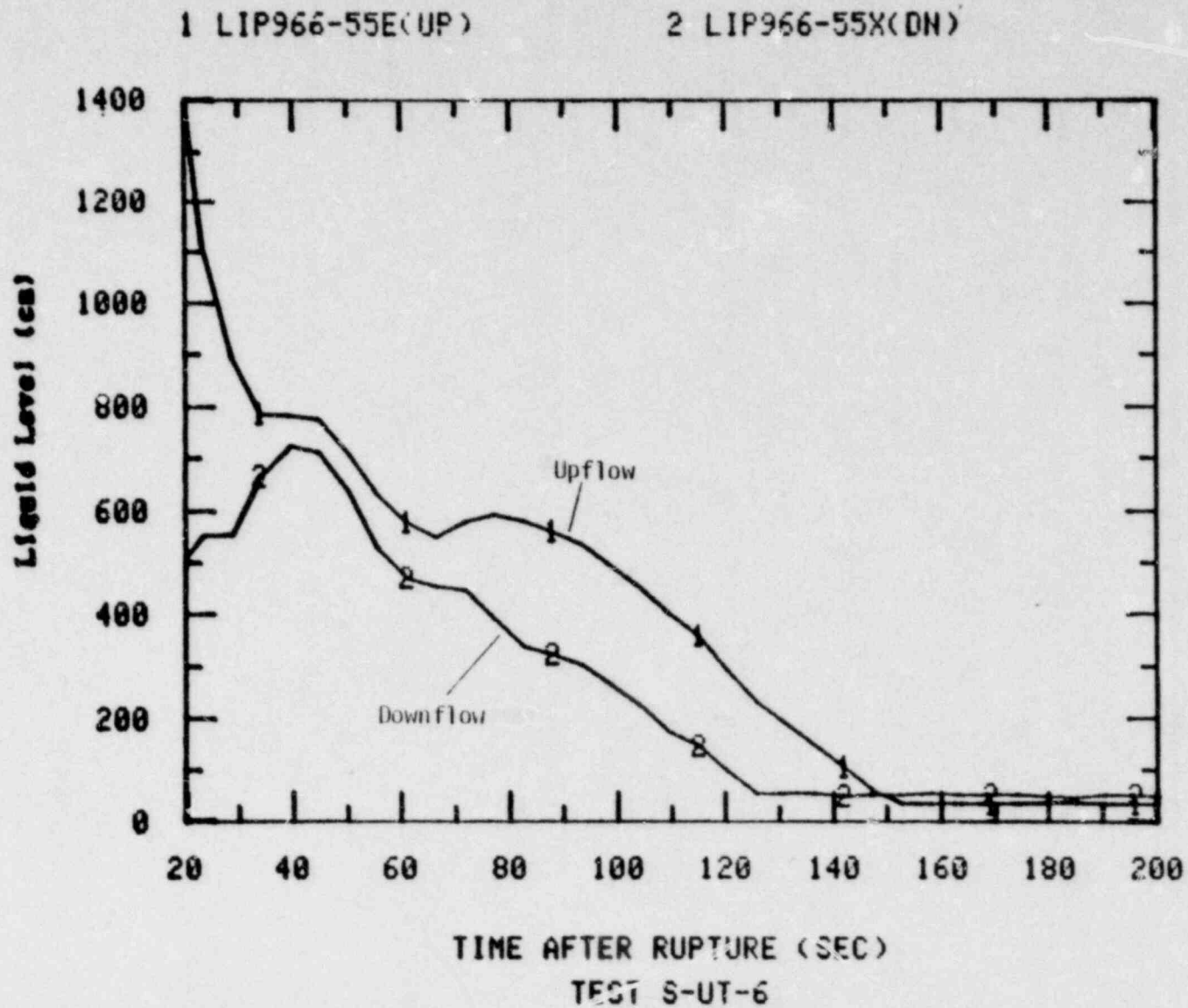


Figure 19. Collapsed liquid levels in the upflow and downflow sides of the intact loop steam generator.

1 BLSG 835-55X(DN)

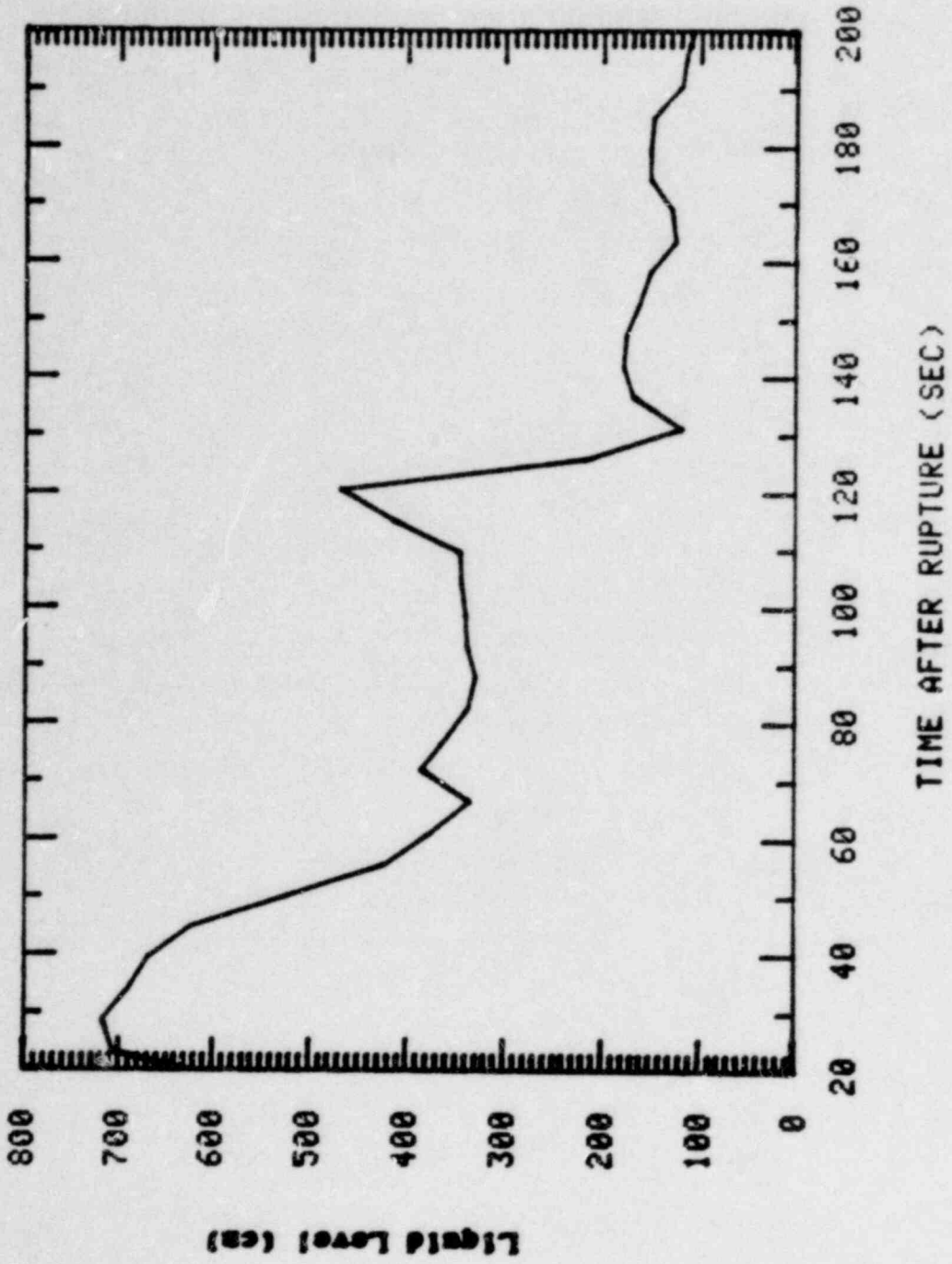


Figure 20. Collapsed liquid level in the downflow side of the broken loop steam generator.

upflow side of the broken loop steam generator appears to have held up some liquid in the tubes until about 250 s.^a

The vessel upper head did not exhibit significant draining until the system pressure dropped to the saturation pressure of the upper head fluid. Figure 21 compares fluid temperatures at several elevations in the upper head with the saturation temperature, and indicates that the fluid became saturated at about 70 s. As the fluid became saturated, the resulting flashing caused liquid to be forced out of the upper head through the guide tube and support columns into the upper plenum, and through the upper head bypass line into the downcomer. Figure 22 shows the upper head collapsed liquid level, and indicates a steady and continuous drain between about 70 and 210 s when it was essentially empty.

As the primary system liquid continued to be lost out the break, the downflow legs of the pump suction legs began to void. Figures 23 and 24 compare the liquid levels in the downflow and upflow legs of the intact and broken loop pump suction legs, respectively. Liquid in the pump suction piping formed a seal which impeded steam flow around the loops, resulting in a somewhat higher pressure in the upper plenum/hot leg region than existed near the break. This caused a slight depression of the mixture level in the vessel, although (as discussed in Section 3.5) no uncovering of the core was observed at this time. At about 210 s, the liquid level in the intact loop pump suction reached the bottom of the downflow leg, and the upflow leg began to clear out providing a steam path around the loop. The resulting pressure equalization between the upper plenum/hot leg region and the break location allowed the core liquid level to rise, and also diminished the driving force to clear the broken loop pump suction. As a result, the loop seal in the broken loop was not blown out as occurred in the intact loop, but rather the liquid levels in the suction leg

a. Although the liquid level measurement on the upflow side of the broken loop steam generator failed during the test, a level measurement in the pantleg (vertical section of pipe just below the steam generator inlet plenum) indicates that the upflow side probably was not completely drained until approximately 250 s.

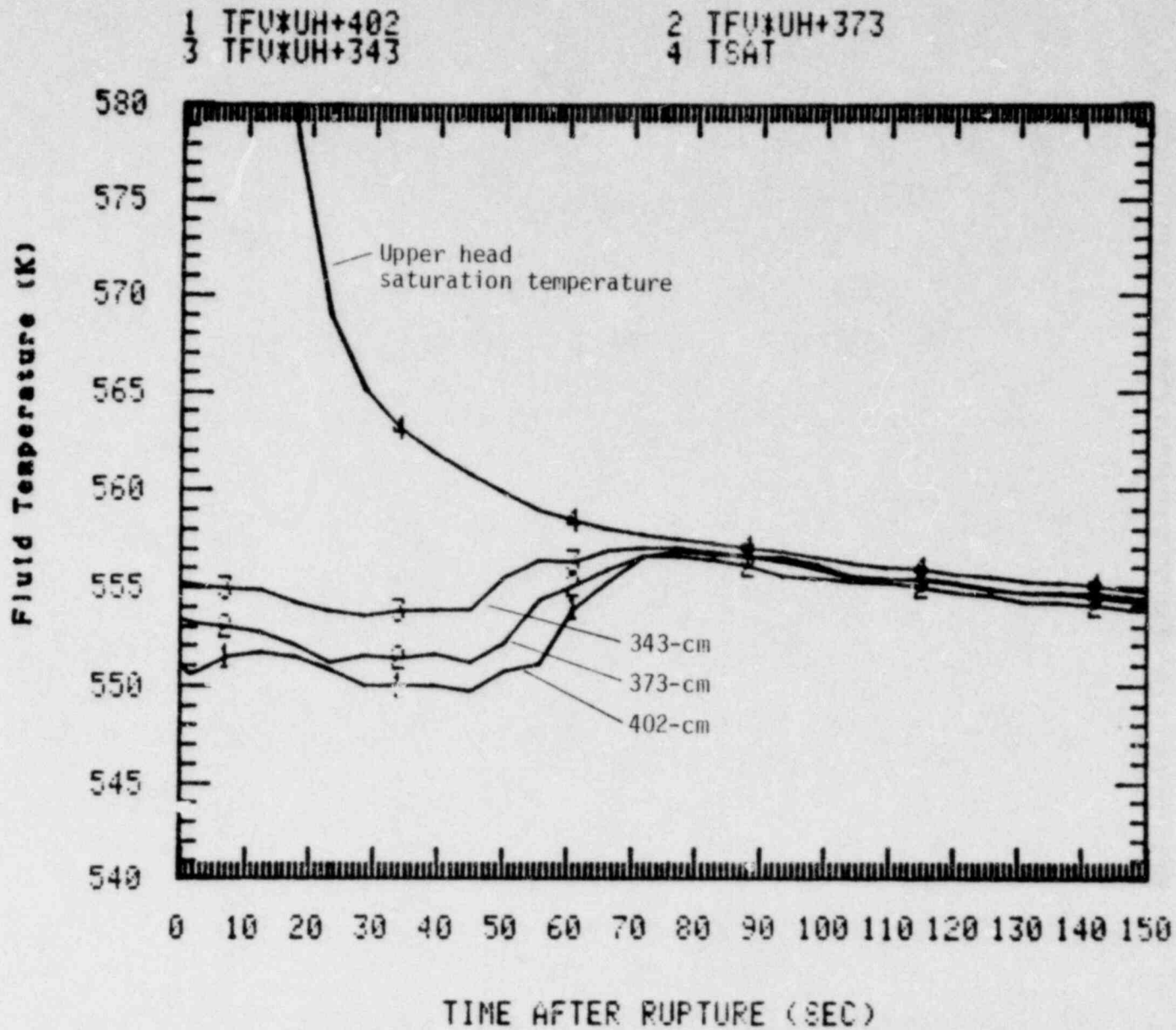


Figure 21. Comparison of upper head fluid temperatures with the saturation temperature (elevations above cold leg centerline).

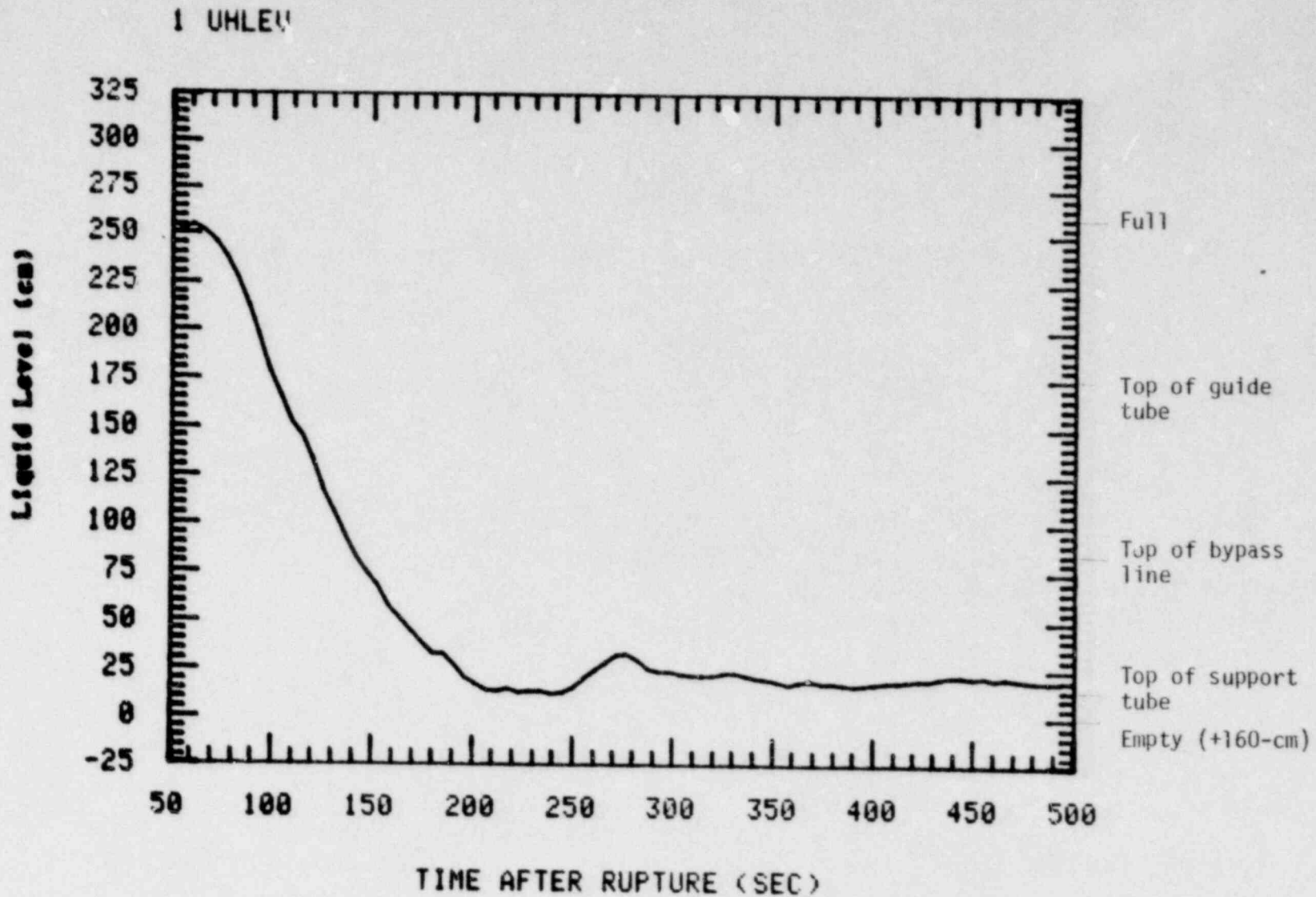


Figure 22. Upper head collapsed liquid level.

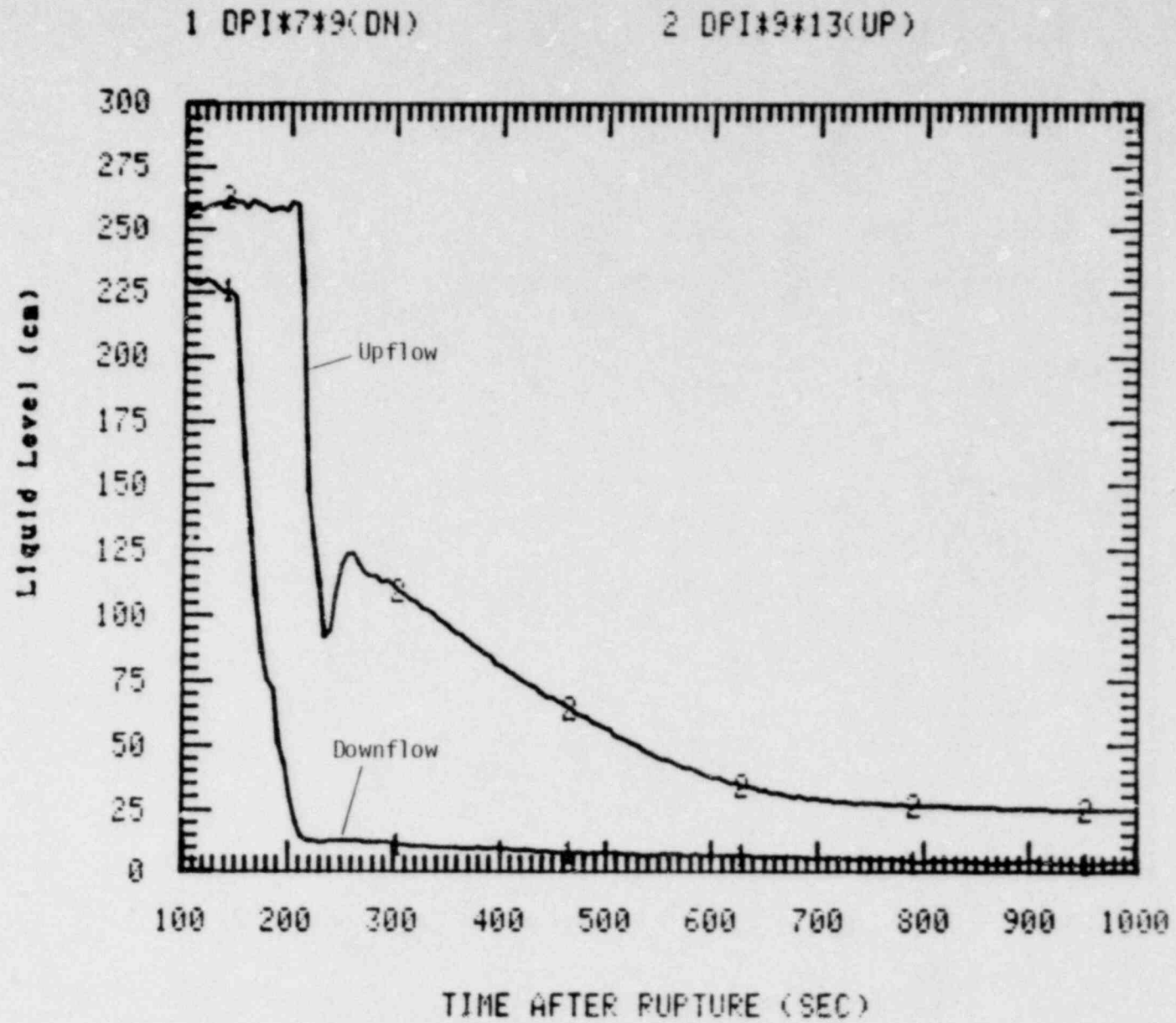


Figure 23. Collapsed liquid levels in the upflow and downflow legs of the intact loop pump suction.

1 DPB#27#28

2 DPB#28#37B

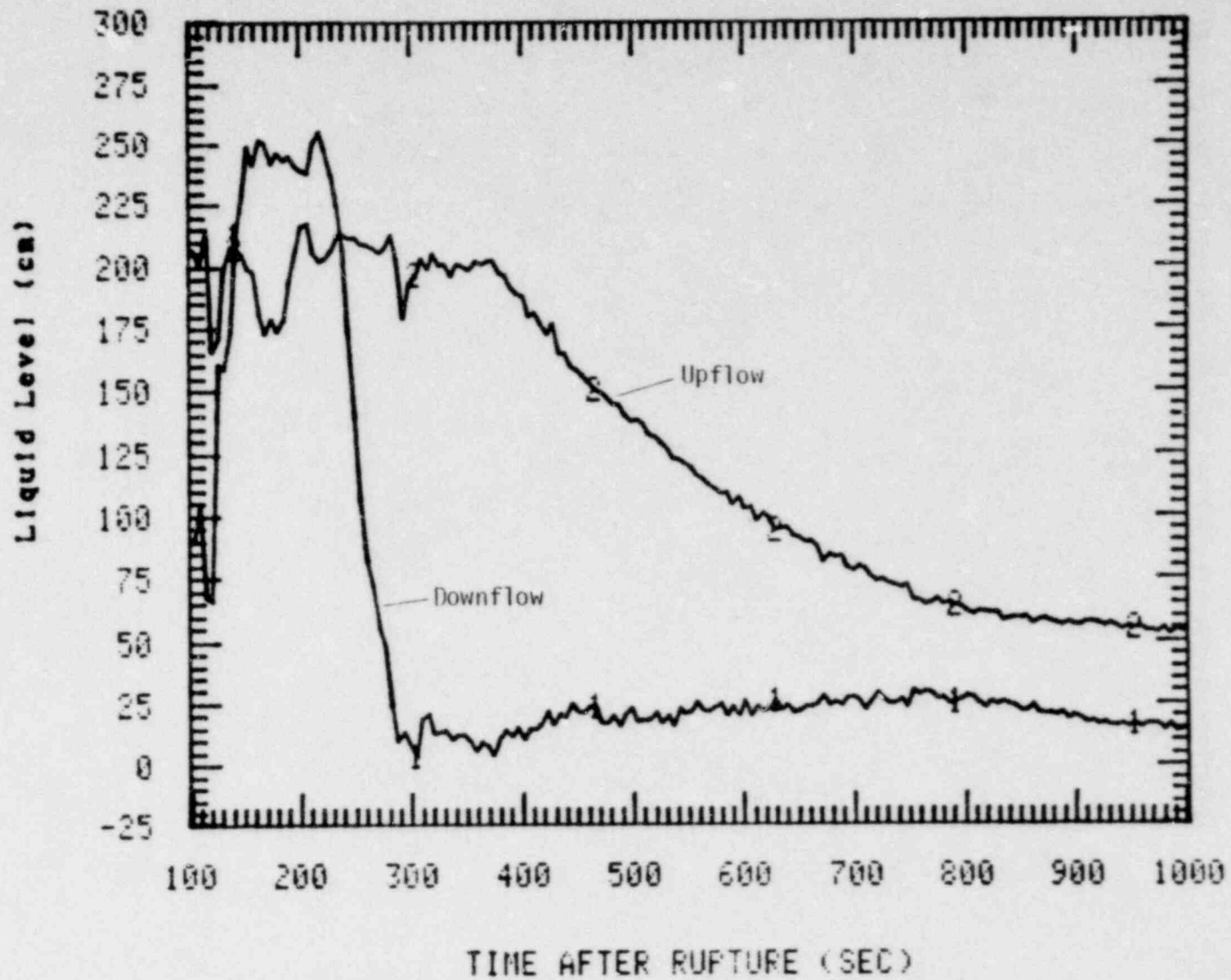


Figure 24. Collapsed liquid levels in the upflow and downflow legs of the broken loop pump suction.

(especially the upflow leg) exhibited a gradual decrease which is indicative of a slow boiloff of the liquid.

After the intact loop seal blew out and the break became uncovered, mass loss from the system was primarily via steam flow out the break. During the period prior to accumulator injection, the cold legs remained essentially voided except for some HPIS liquid in the bottom of the intact loop pipe. Figure 25 shows the fluid density in the intact loop cold leg near the vessel. The magnitude of the density during the period between 220 and about 750 s is indicative of a stratified layer of liquid in the bottom of the pipe. Since the broken loop HPIS did not operate for the test, the broken loop cold leg density measurement showed a steam environment during the same period (Figure 17). As indicated previously some liquid did remain in the upflow leg of both the intact and broken loop cold leg during this period (Figures 23 and 24), although a gradual boiloff of the liquid was occurring. Also, a relatively high steam flow out the top of the core (Figure 26), tended to hold up a considerable amount of liquid in the hot legs. Figures 27 and 28 show the fluid densities in the intact and broken loop hot legs, respectively, and indicate the presence of liquid between 220 and 750 s.

The intact and broken loop accumulators began injecting liquid into the cold legs at about 730 and 750 s, respectively. Essentially all the intact loop accumulator liquid flowed into the downcomer and began refilling the downcomer and core region, although as indicated previously, most of the broken loop accumulator exited the system via the break. The system filled sufficiently, however, with the intact loop accumulator injection to have high density fluid in the intact and broken loop hot legs by about 1250 s (Figures 27 and 28). Some liquid also collected in the bottom of the vessel upper head after about 1600 s. By the time the intact loop accumulator flow was terminated (about 2800 s), the break flow rate had dropped below the HPIS flow rate, and the primary system mass inventory continued to increase for the duration of the transient.

1 RI*17B

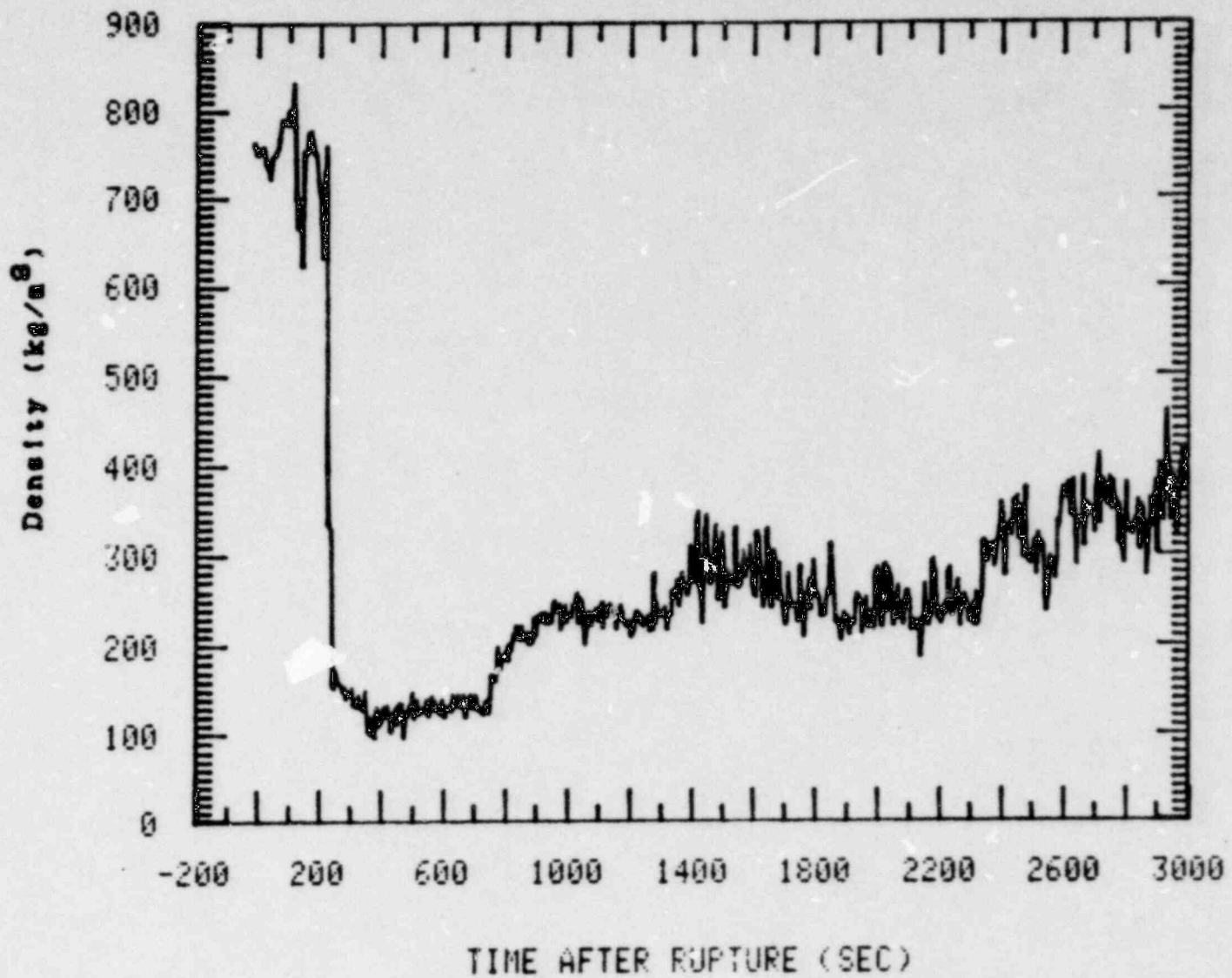


Figure 25. Fluid density in the intact loop cold leg near the vessel.

1 QU*UP+1

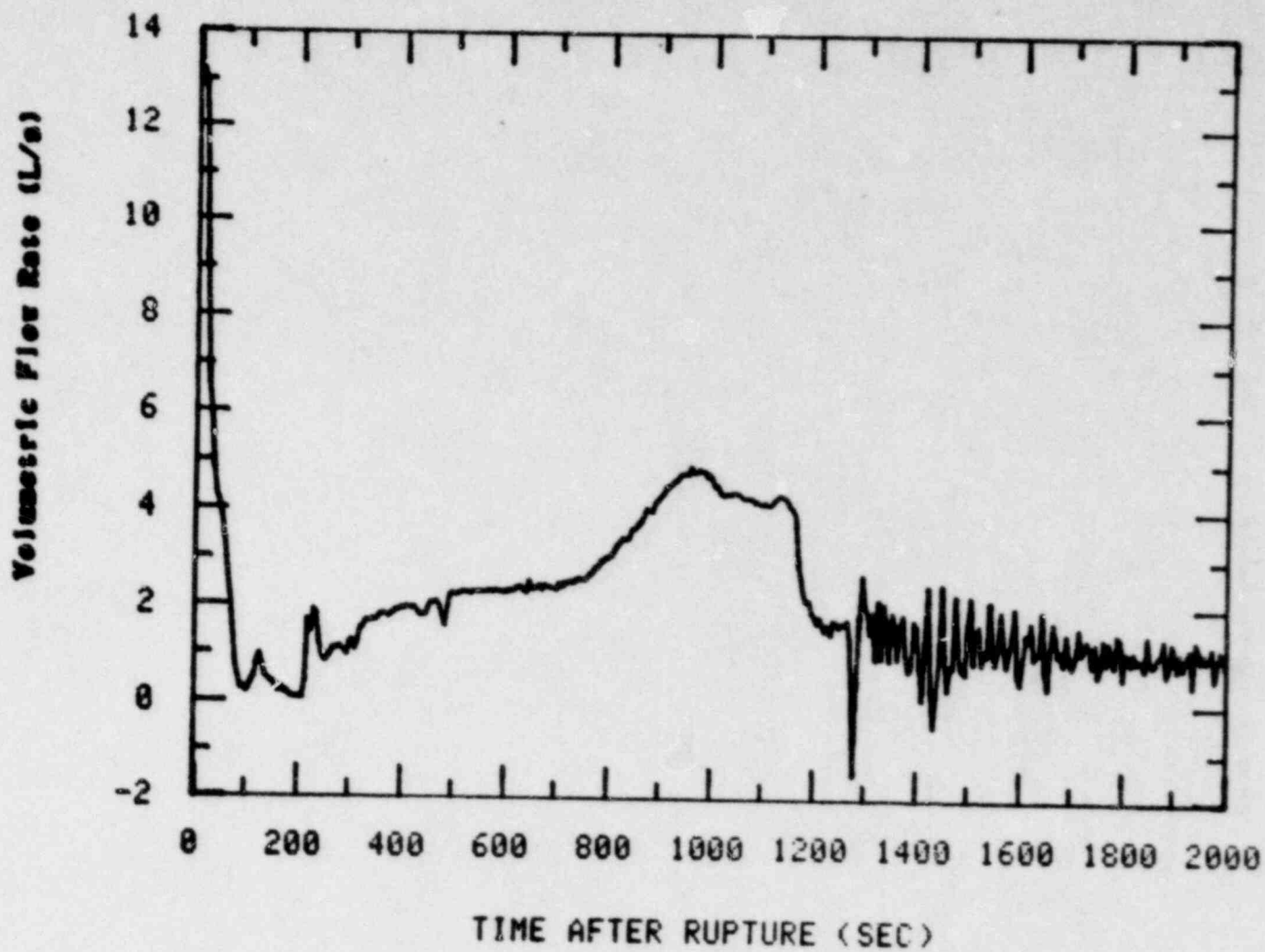


Figure 26. Volumetric flow in the vessel upper plenum.

1 RI*1B

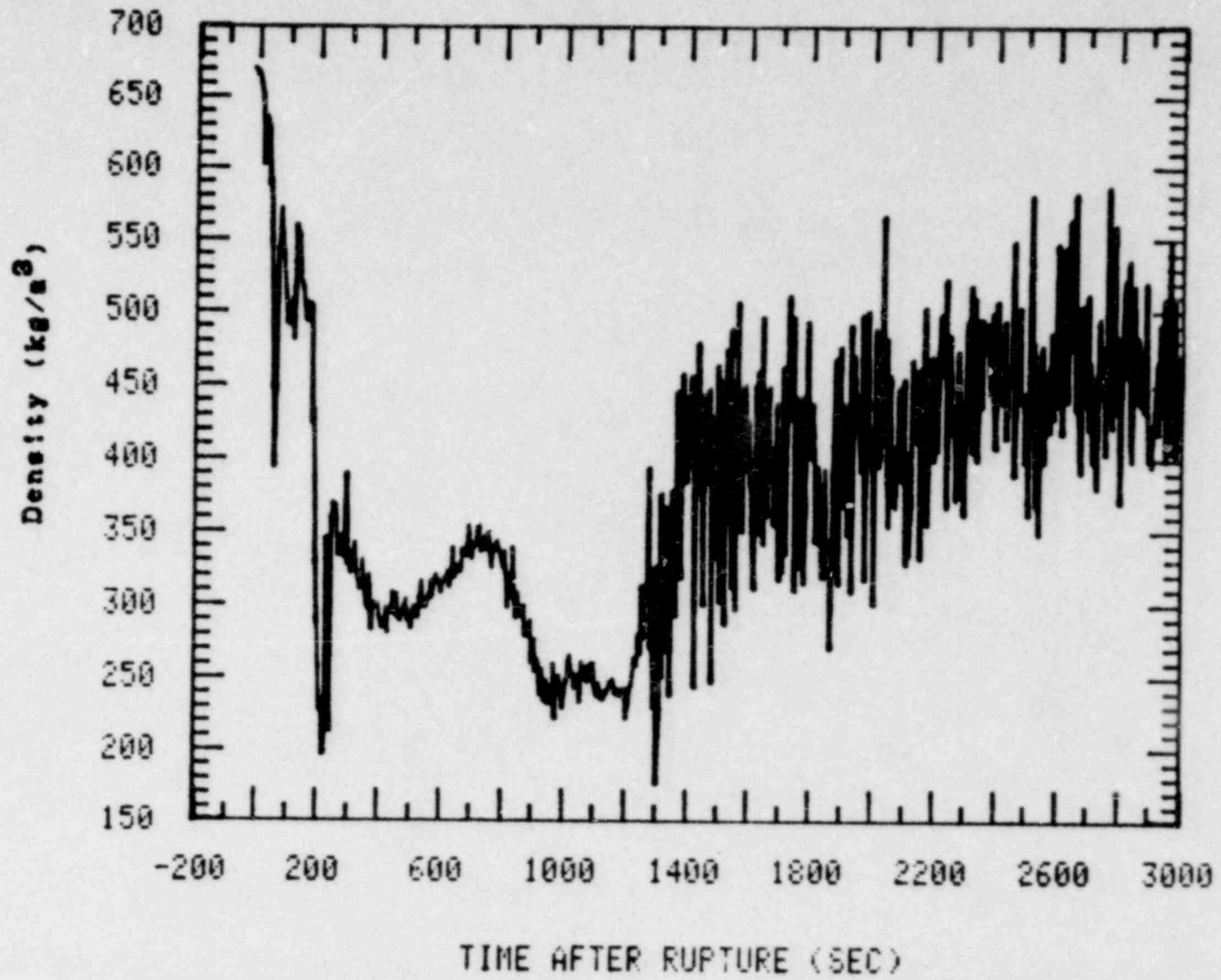


Figure 27. Fluid density in the intact loop hot leg.

1 RB*20B

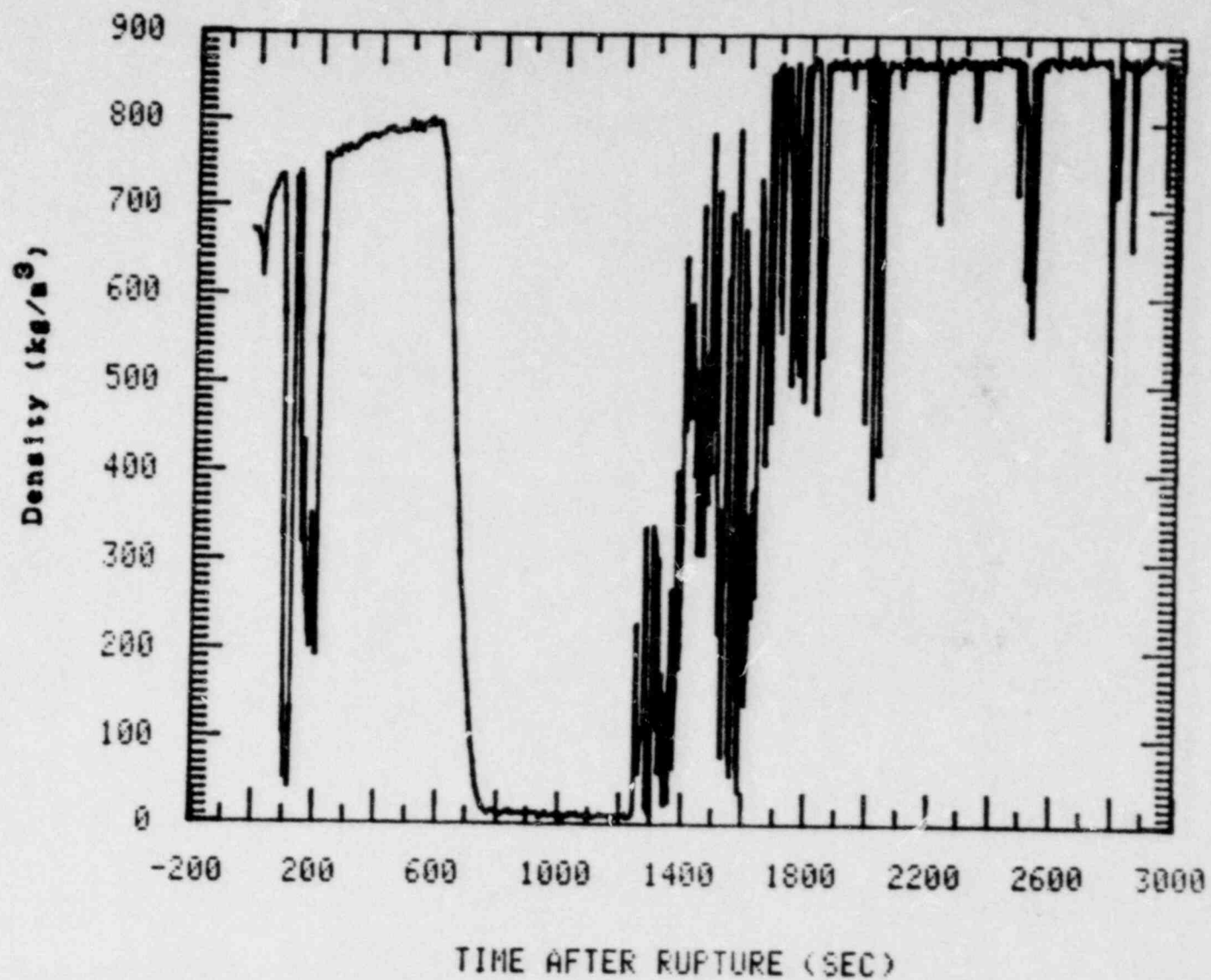


Figure 28. Fluid density in the broken loop hot leg.

A preliminary analysis was made to perform an overall mass balance on the system by taking into account the mass flow rates into and out of the system. The mass flow out of the system (break flow and leakage)^a was subtracted from flow into the system (HPIS and intact and broken loop accumulator flows). This net mass flow rate was integrated and added to the 155 kg initial system mass. The resulting transient system mass is shown in Figure 29, and is compared with a mass inventory based on liquid levels in the vertical sections of the system.^b As indicated in the figure, the agreement between the two methods of obtaining the transient system mass is quite good during the first 1300 s, although there is considerable divergence between the two methods after that time. However, the transient system mass obtained by the liquid level method does not include any mass residing in the horizontal sections of the system. As indicated earlier, considerable liquid was present in the hot legs after 1250 s, although the limited number of density measurements (one in each hot leg) makes it difficult to determine the actual transient hot leg coolant mass. If the hot leg coolant mass were added to mass obtained from the liquid level method, the agreement between the two transient inventories presented in Figure 29 should be significantly improved. It is thus felt that the mass balance method presented in Figure 29 provides a good measure of the transient system mass inventory, as well as the minimum system inventory reached during the test.

3.5 Core Response

Since the break flow rate during the early part of Test S-UT-6 was significantly greater than the HPIS flow rate, the vessel liquid inventory decreased continuously until the initiation of accumulator injection. The

a. Most of the system leakage occurs through the intact loop pump seals during the first 200 to 300 s when liquid is present in the pump suction region. After this time pump seal leakage should be minimal.

b. Differential pressure measurements were used to calculate collapsed liquid levels in the different regions of the system. The levels were then converted to a mass assuming a saturated liquid density and applying an appropriate cross sectional area.

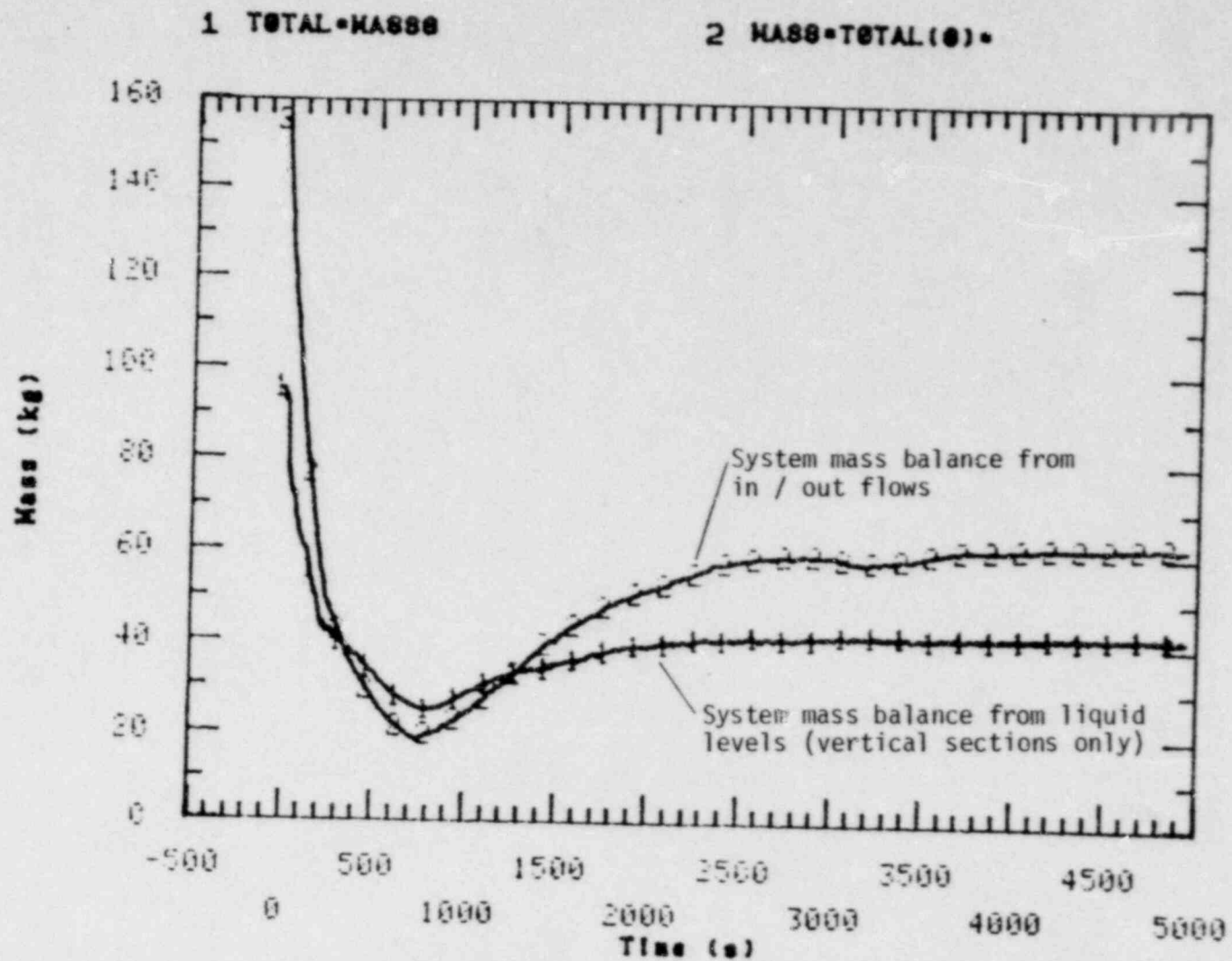


Figure 29. System mass balance using inflow / outflow method and liquid level method.

downcomer and core collapsed liquid levels (obtained from differential pressure measurements) are shown in Figure 30. Immediately following rupture, the core collapsed liquid level exhibited a rapid decrease as boiling in the core led to a rapid increase in void fraction, especially in the upper core region. Figure 31 compares the fluid densities at several elevations in the core. The decreasing densities and large axial gradient of two-phase fluid established early in the test are indicative of the continuous boiling and void formation occurring in the core region.

As the upper head began to drain at about 70 s, liquid entering the upper plenum gave rise to a brief increase in the core level (Figure 30). However, as the liquid seals in the pump suction began to form, the steam generated in the core was restricted from flowing freely around the loops to the break. The resulting increase in differential pressure between the vessel upper plenum and break location caused a further depression of the core collapsed liquid level, although no uncovering of the core was observed during the period the loop seals were present. The blowout of the intact loop seal at about 210 s, allowed equalization of the pressure between the vessel upper plenum and break location giving rise to the relatively rapid (although not significant in terms of core cooling) rise in core level shown in Figure 30.

After blowout of the liquid seal in the intact loop occurred, a slow boiloff of the core fluid began causing a steady decrease of the vessel/downcomer liquid inventory. The boiloff continued until by about 560 s the vessel mixture level dropped below the top of the core. Figure 32, which compares fluid densities in the upper half of the core, indicates significant uncovering of the core occurred during the period between 560 and about 1000 s. Some typical heater rod cladding temperatures showing the temperature excursion which occurred as a result of dryout, are presented in Figure 33. The peak cladding temperature during the dryout period was about 660 K, which is somewhat lower than the normal steady state operating temperature of the cladding. When accumulator injection began at about 720 s, a steady refilling of the core occurred, and the resulting increased steam flow through the upper part of

1 DCLL +29-578

2 CORE LL 578-13M

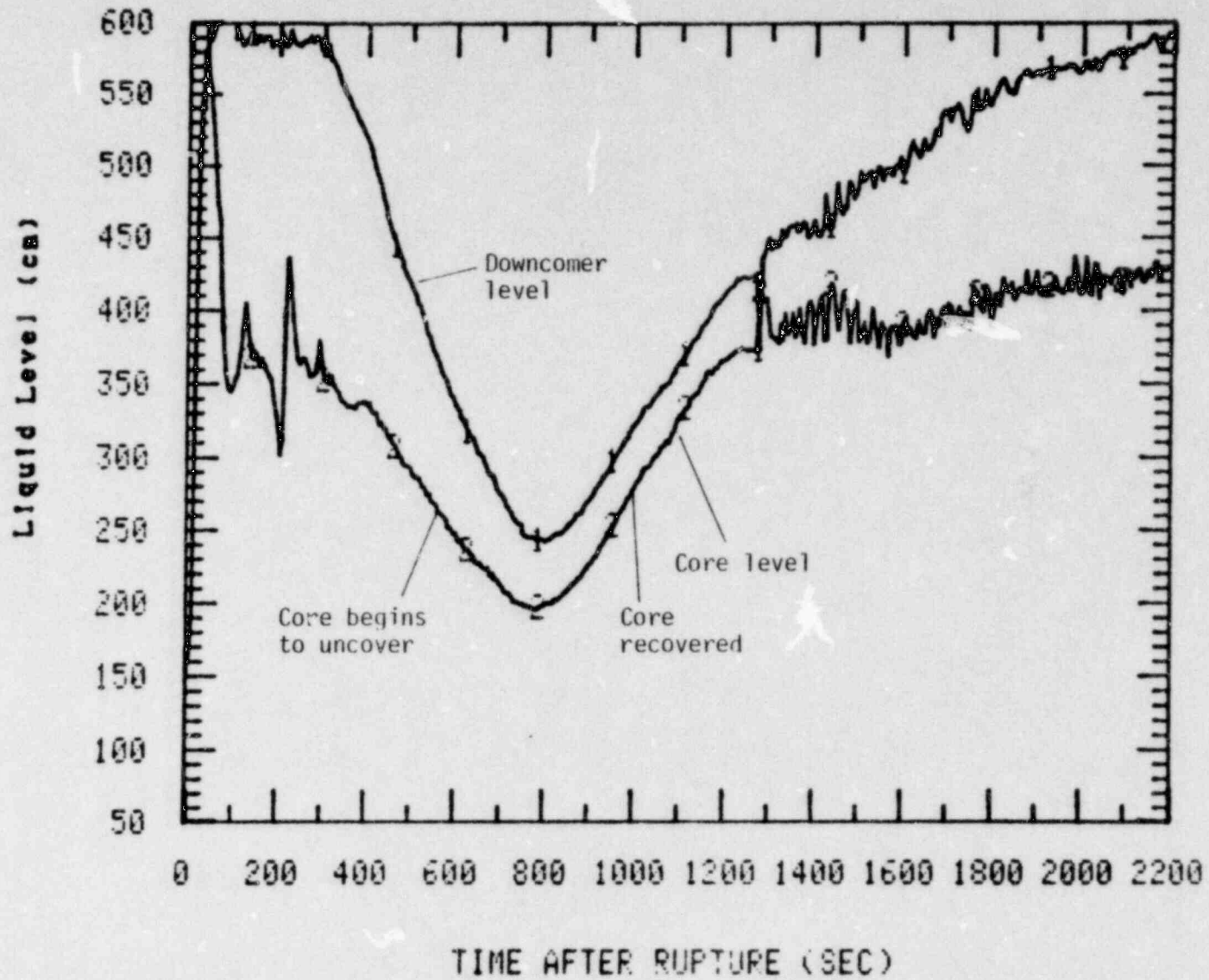


Figure 30. Downcomer and core collapsed liquid levels.

1 RU#23+342
3 RU#23+113

2 RU#23+253

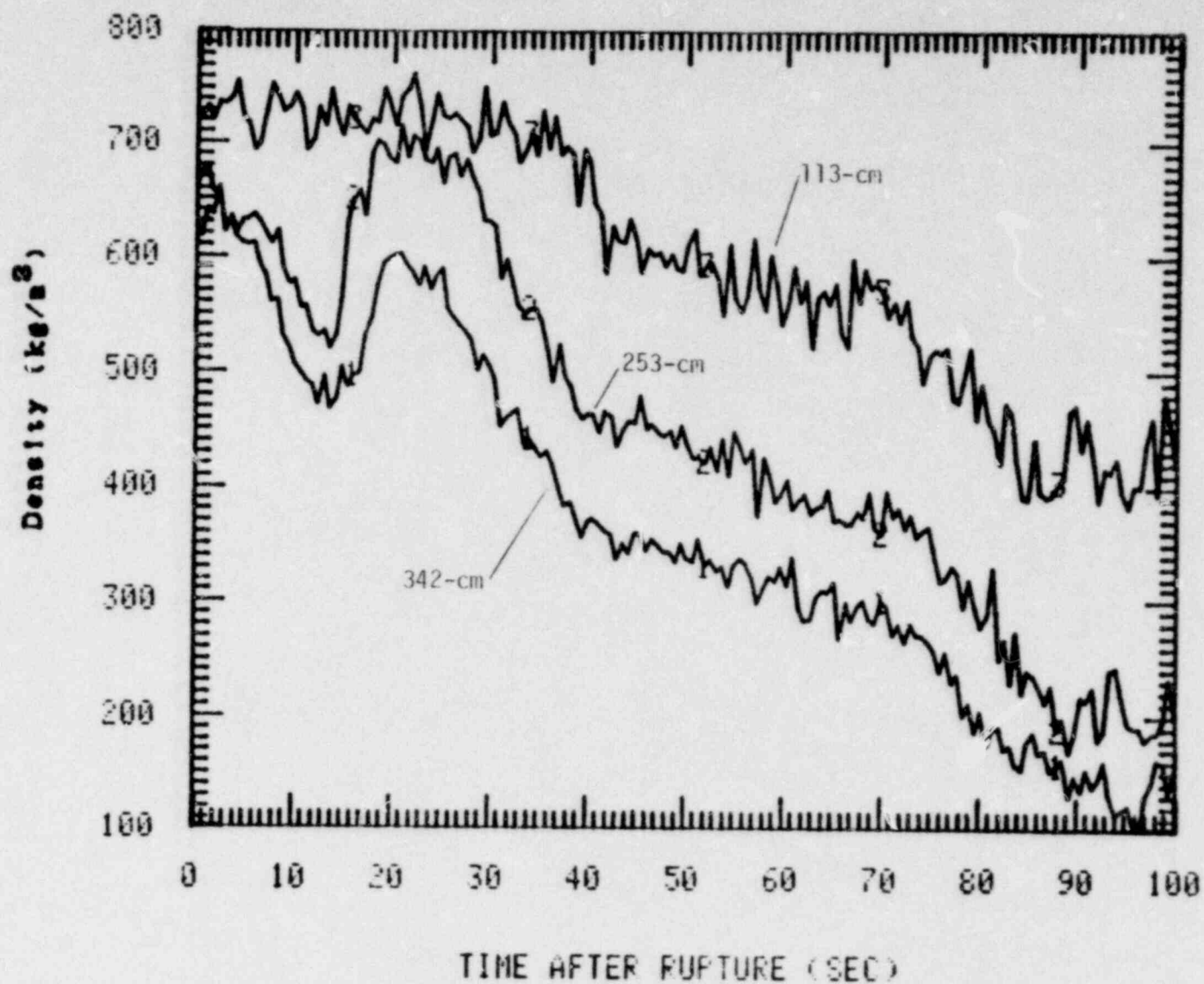


Figure 31. Fluid densities in the core (elevations above bottom of core).

1 RU#23+183
3 RU#23+342

2 RU#23+253

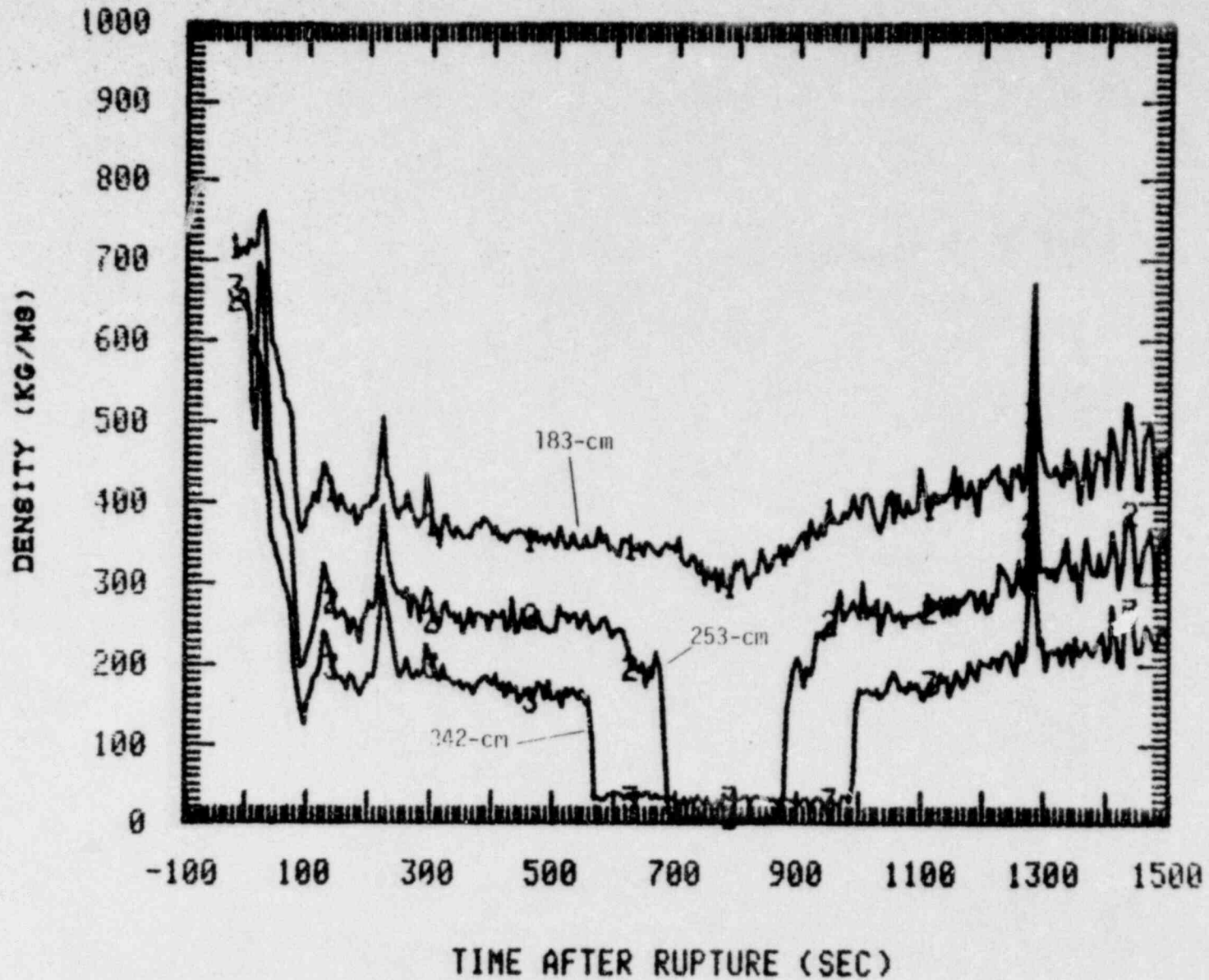


Figure 32. Fluid densities in upper half of core illustrating uncovering as result of boiloff (elevations above bottom of core).

1 THU*B4+322
3 THU*B1+183

2 THU*A3+291

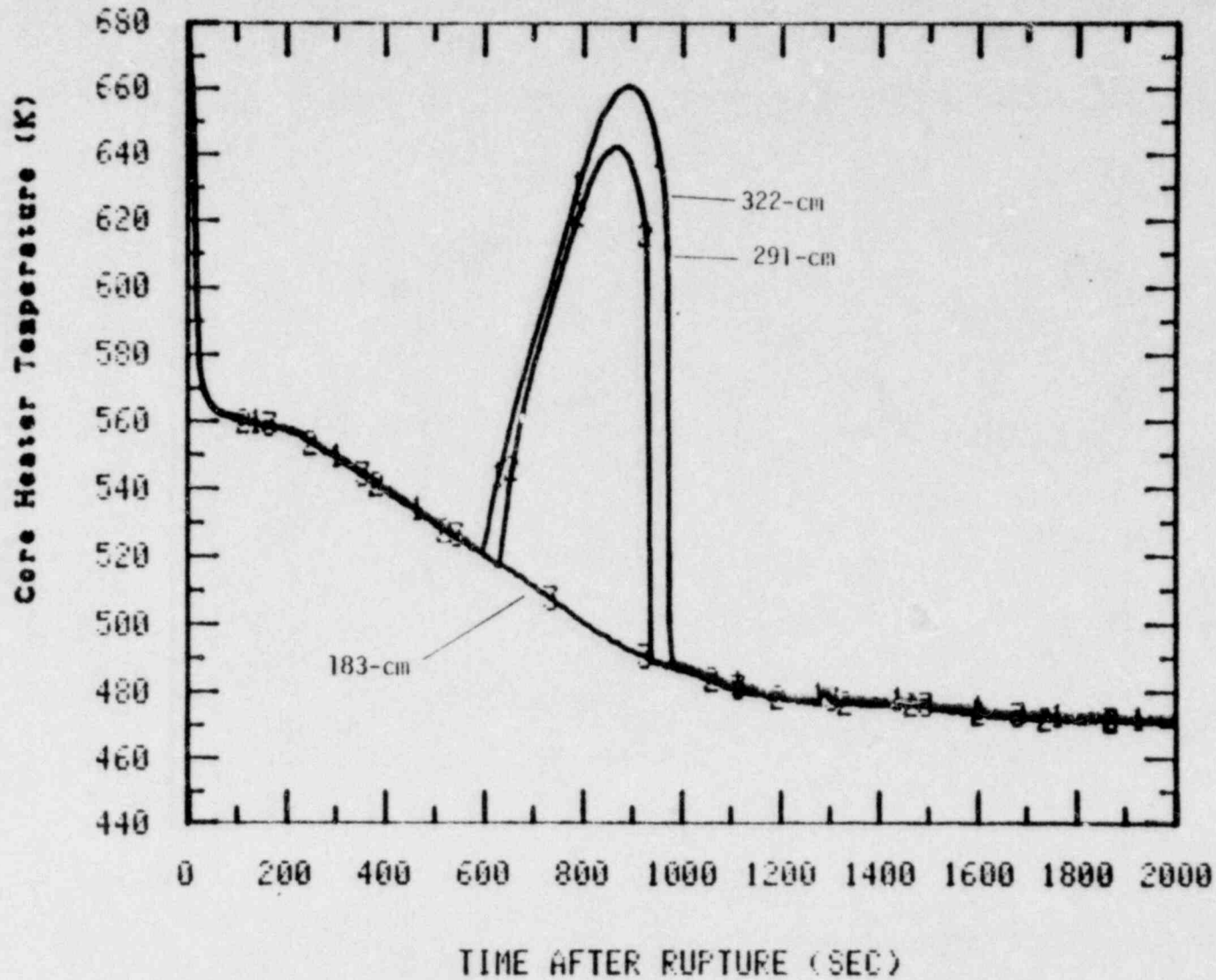


Figure 33. Heater rod cladding temperatures illustrating temperature excursion in upper part of core (elevations above bottom of core).

the core terminated the temperature excursion by about 900 s. The core was completely recovered by about 1000 s. After all the accumulator liquid had been injected (by 2800 s), the HPIS adequately replenished core boiloff and, in fact, was sufficient to provide a slowly increasing primary system liquid mass.

4. COMPARISON OF SELECTED DATA TO PRETEST PREDICTION CALCULATION

A comparison of Test S-UT-6 data to results of the test prediction is presented in this section. The test prediction calculation was performed through the first 840 s of the transient using the RELAP5/MOD1 computer code (Version 6). A detailed description of the results of the calculation is given in Reference 4. The system model used in the calculation is discussed in Appendix A. Comparisons presented in this section provide a basis for evaluating the capability of the present analytical model to predict the system response resulting from a 5.0% communicative cold leg break in the Semiscale Mod-2A facility. Table 3 compares the significant initial conditions specified, measured, and calculated for Test S-UT-6.

The primary system pressure response is compared to the test prediction in Figure 34. The calculation shows good agreement during the period 0-200 s. This was prior to the onset of pump seal clearing. During this initial time interval the calculated system pressure was slightly above the test response. The initial overprediction of system pressure is partially a result of the intact loop steam generator secondary mass being greater than that modeled in the calculation. Therefore, the intact loop steam generator secondary side was calculated to be too small a heat sink. Consequently, the calculation initially overpredicted the intact loop cold leg temperature (Figure 35a), and therefore saturation pressure, as well as the secondary side temperature and pressure responses shown in Figures 36a and 36b, respectively. As a result, the calculated primary system pressure was higher than the test response. The initial calculated temperature and pressure responses of the broken loop secondary (Figures 36a and 36b) were in good agreement with the test data. An initial overprediction in the broken loop cold leg temperature did not occur (Figure 35b).

After 200 s the calculated system pressure began to significantly diverge from the test response (Figure 34). The calculated system pressure began to be underpredicted at the time that significant clearing of the

TABLE 3. INITIAL CONDITIONS FOR TEST S-UT-6

	<u>Specified</u>	<u>Measured</u>	<u>RELAP5</u>
Pressurizer pressure (MPa)	15.5 ± 0.2	15.6	15.5
Hot leg fluid temperature (K)	594 ± 2	597	594
Cold leg fluid temperature (K)	557 ± 2	557	557
Total core power (MW)	2.0 ± 0.005	2.0	2.0
Core inlet flow rate (kg/s)	9.77 ^a	8.5	9.3
Steam generator secondary pressure (MPa)			
Intact loop	5.85 ± 0.18	5.7	5.7
Broken loop	5.85 ± 0.18	5.9	5.6
Steam generator secondary water level (m)			
Intact loop	-- ^b	10.4	4.8
Broken loop	-- ^b	8.1	6.8

a. Approximate value; flow is adjusted to achieve required core ΔT .

b. Secondary side levels are specified to be adjusted to obtain required primary side ΔT .

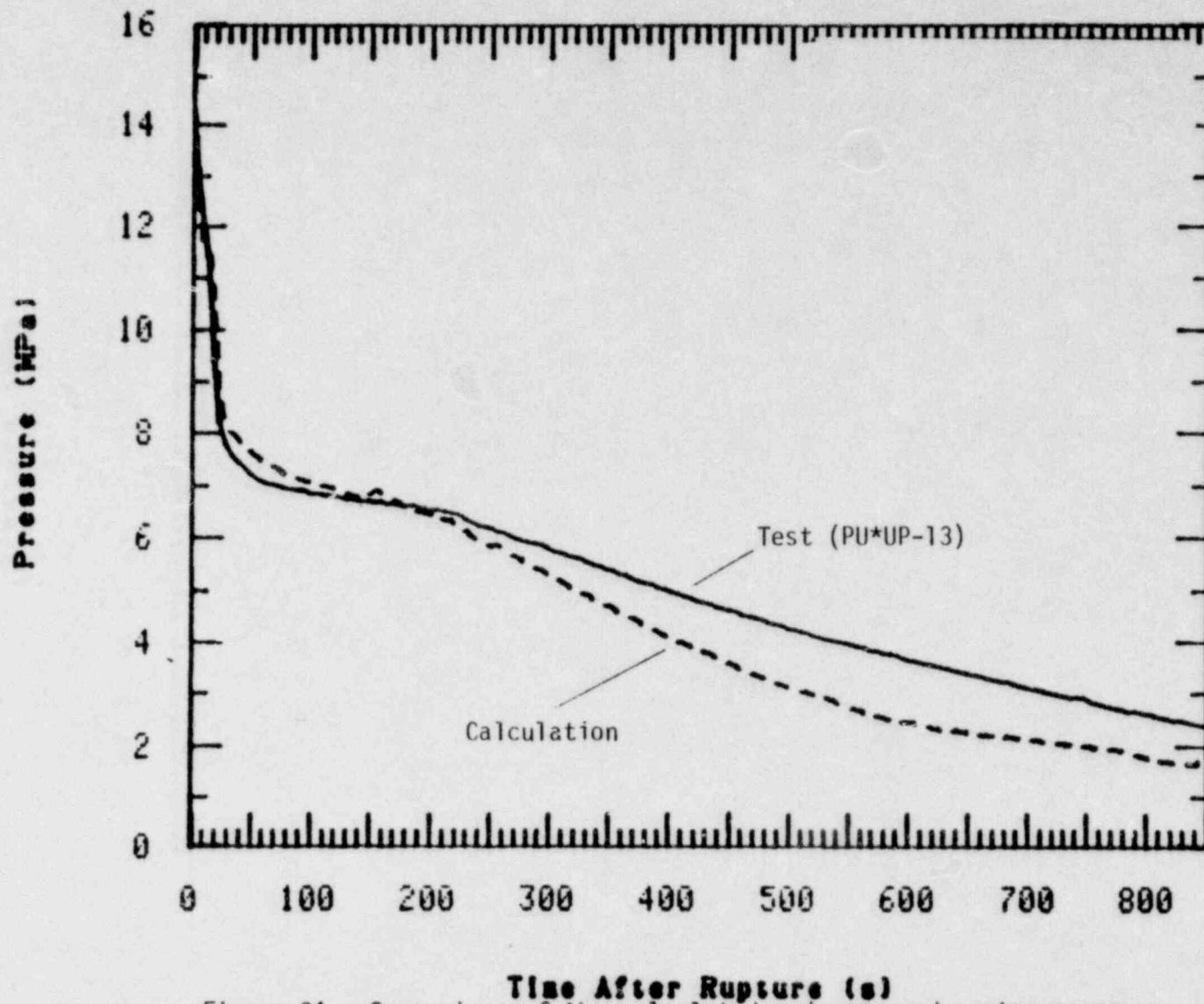
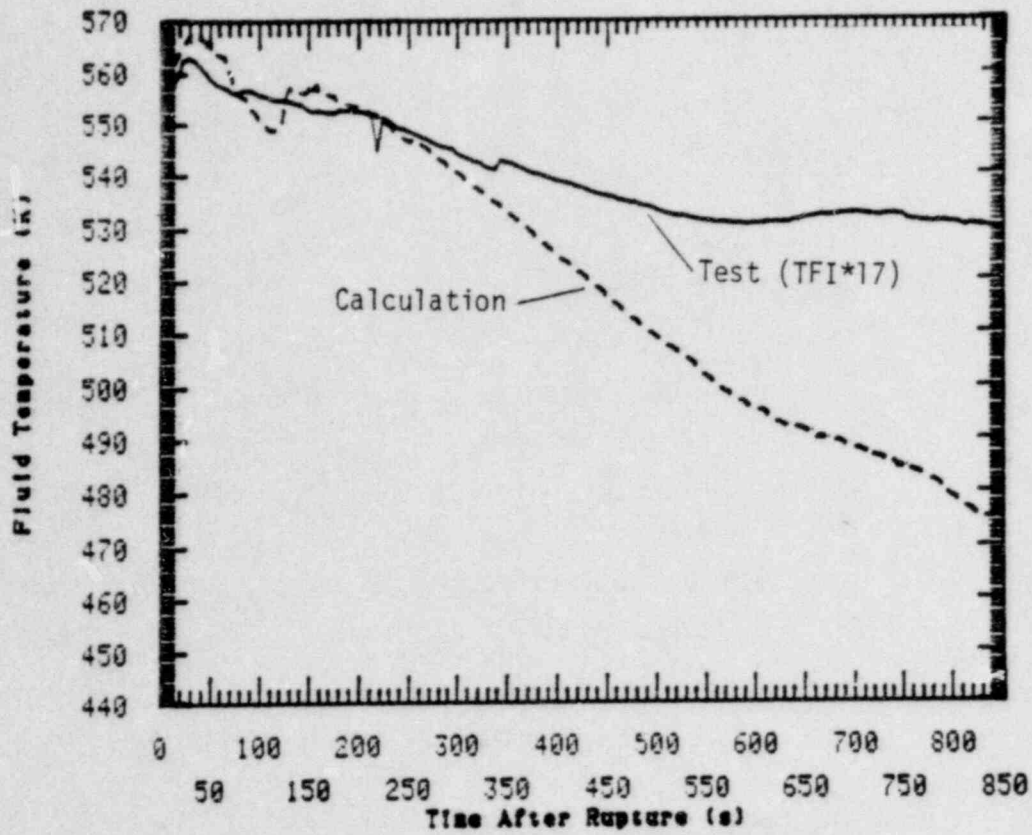
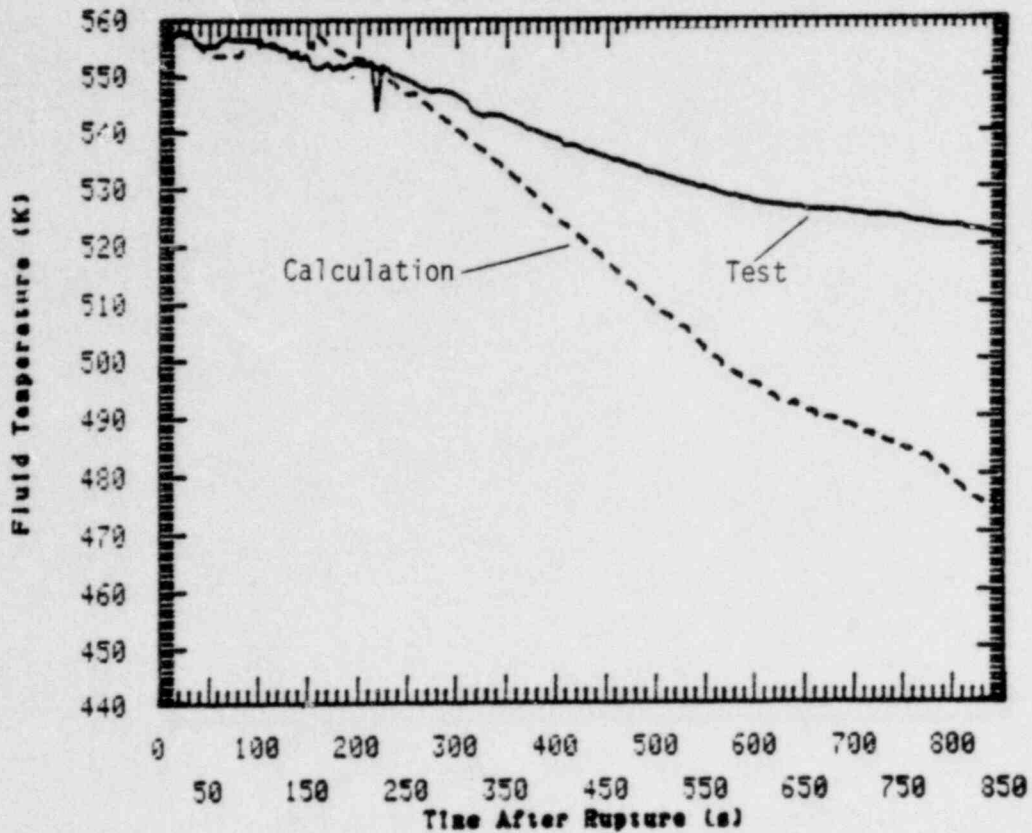


Figure 34. Comparison of the calculated and measured system pressure response for Test S-UT-6.



(a) INTACT LOOP COLD LEG TEMPERATURE



(b) BROKEN LOOP COLD LEG TEMPERATURES

Figure 35. Comparison of the calculated and measured cold leg temperatures for Test S-UT-6.

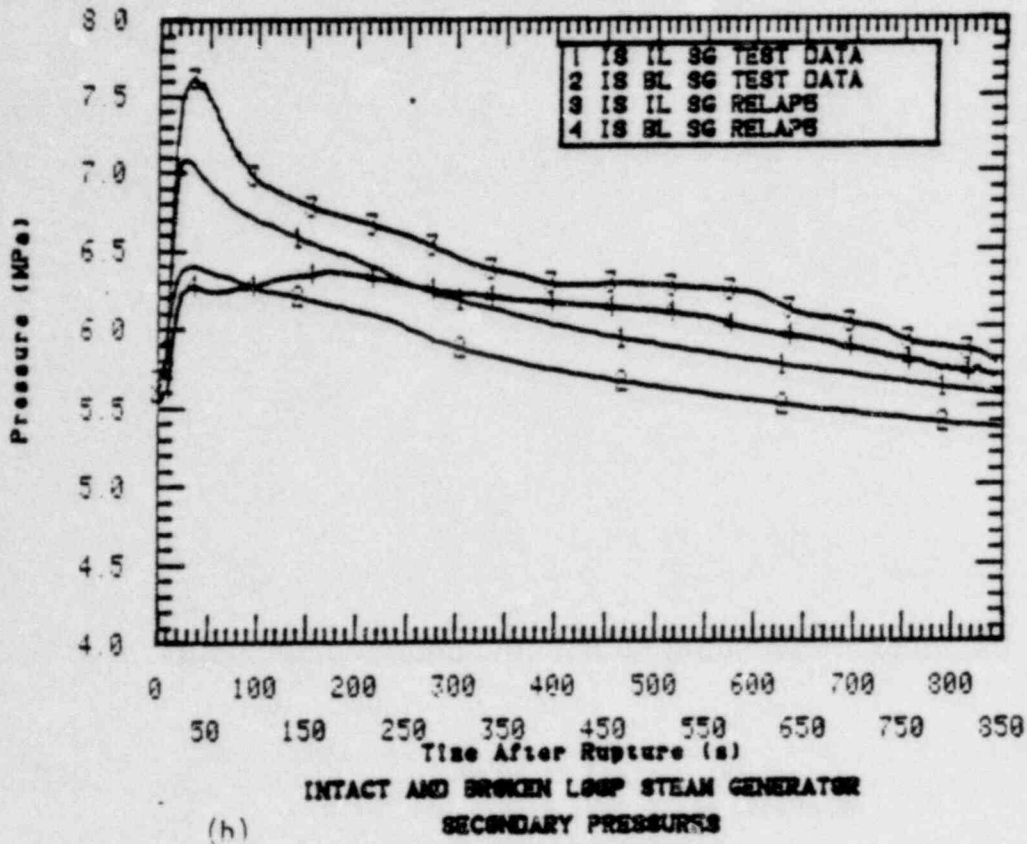
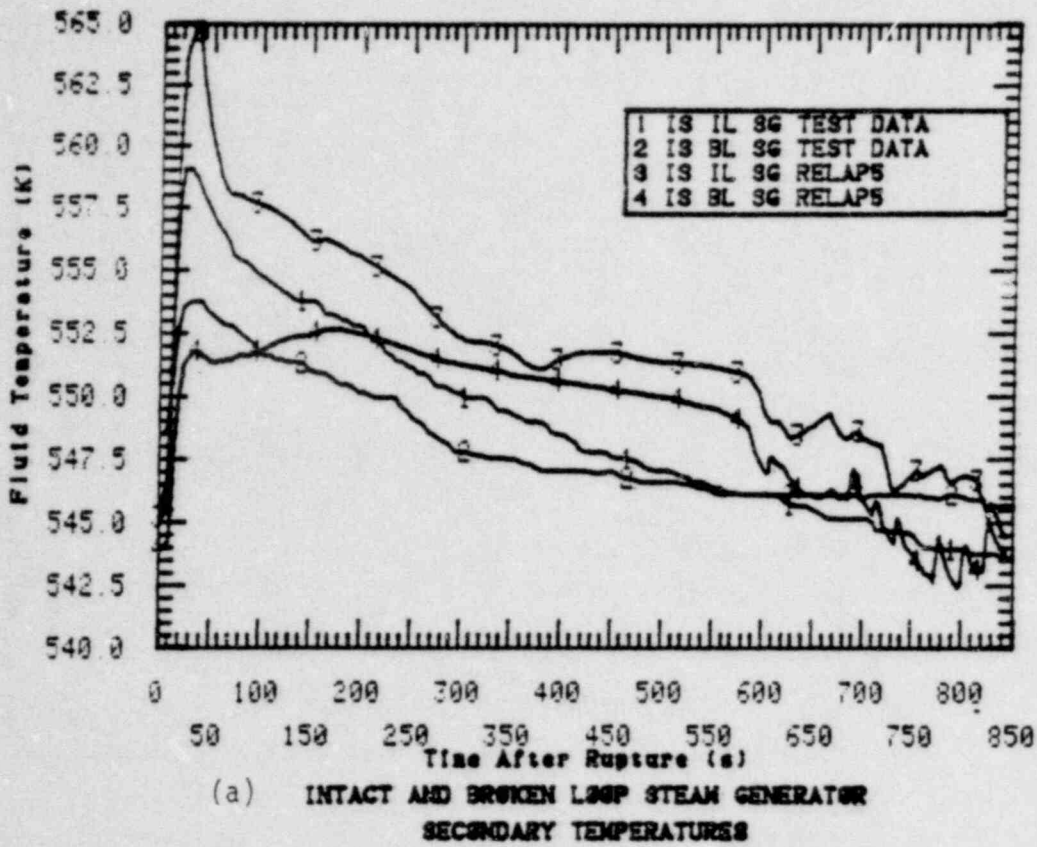


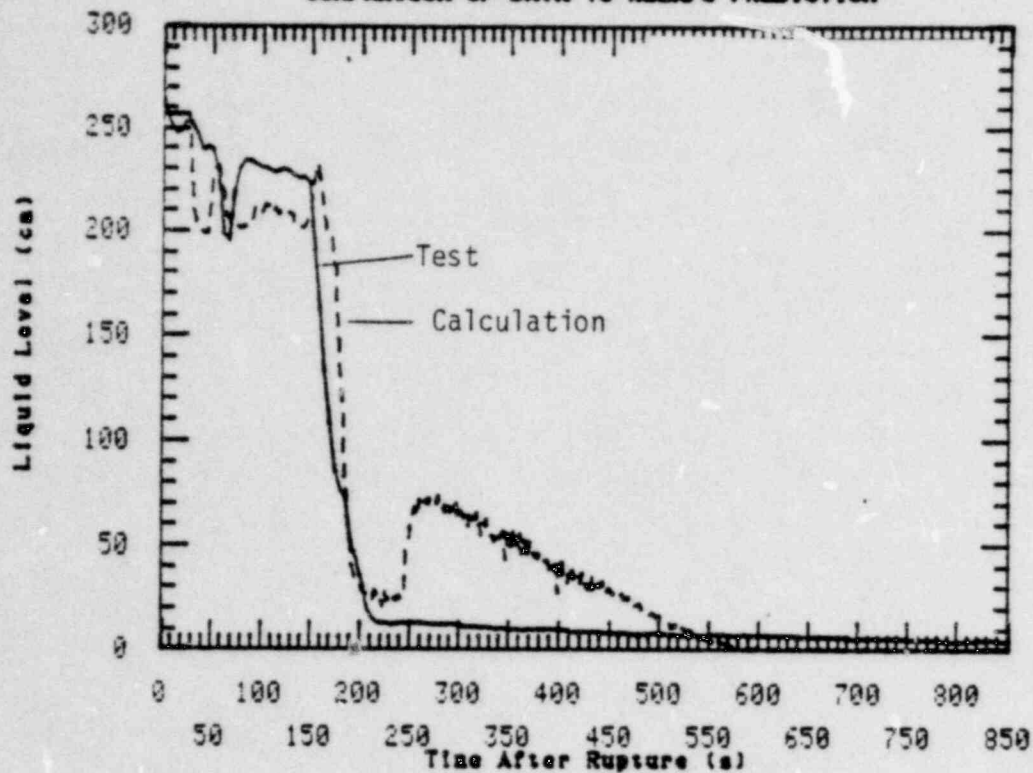
Figure 36. Comparison of the calculated and measured steam generator secondary fluid temperatures and pressures for Test S-UT-6.

intact and broken loop pump suction seals occurred. A comparison of the calculated and measured intact and broken loop pump suction downflow and upflow collapsed liquid levels are presented in Figures 37a-b and 38a-b, respectively. The intact and broken loop downflow sides were calculated to clear at approximately 200 s. However, partial refilling did occur in the intact loop. In the experiment the intact and broken loop pump suction levels for the downflow side cleared at 200 s and 300 s respectively. Generally, the calculated liquid levels in both the intact and broken loop downflows, and intact loop upflow were in good agreement with the test data.

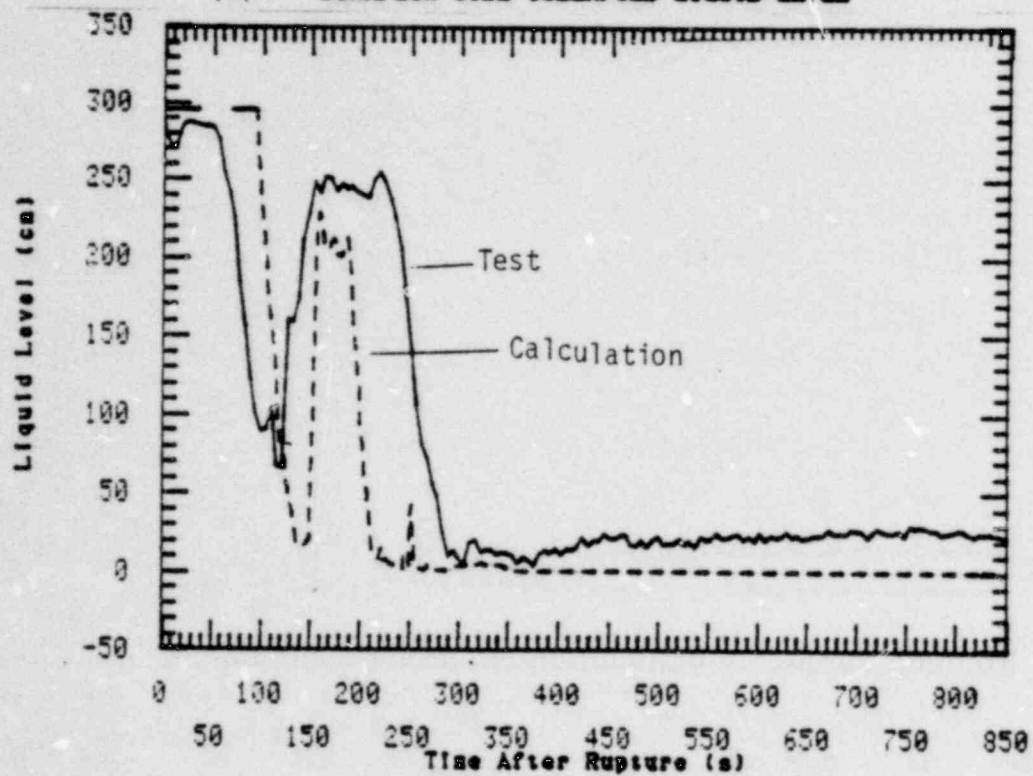
In the calculation, the pump seal clearing created a vapor path to the break which resulted in increased volumetric flow at 200 s. As a consequence, the calculated depressurization was increased. A similar but smaller increase in depressurization occurred in the test after loop seal clearing began.

The predicted and measured hydraulic responses in the vessel are illustrated by the upper head and core collapsed liquid level comparisons shown in Figures 39a and 39b. The upper head liquid drain response was accurately predicted; however, the calculated core level response was significantly underpredicted. The underprediction in the core level is attributed to two principal reasons. First is the overprediction of break flow rate. Figure 40 compares the measured cumulative discharge to the calculated integrated break flows. The resulting overprediction in system mass loss leads to an underprediction of core mass inventory and system pressure. The apparent difference between the measured and calculated break flow rates is due to modeling of the break junction with a two-phase discharge coefficient which was too large (0.9 was the value used). The value of the two-phase discharge coefficient is dependent on the break orifice geometry and is not known precisely. The approximate range of values for the orifice geometry used in Test S-UT-6 is between 0.7 and 0.9. The appropriate value of the break two-phase discharge coefficient will be determined during the S-UT-6 posttest analysis effort.

**NECSA SEMISCALE TEST S-UT-6
COMPARISON OF DATA TO RELAPS PREDICTION**

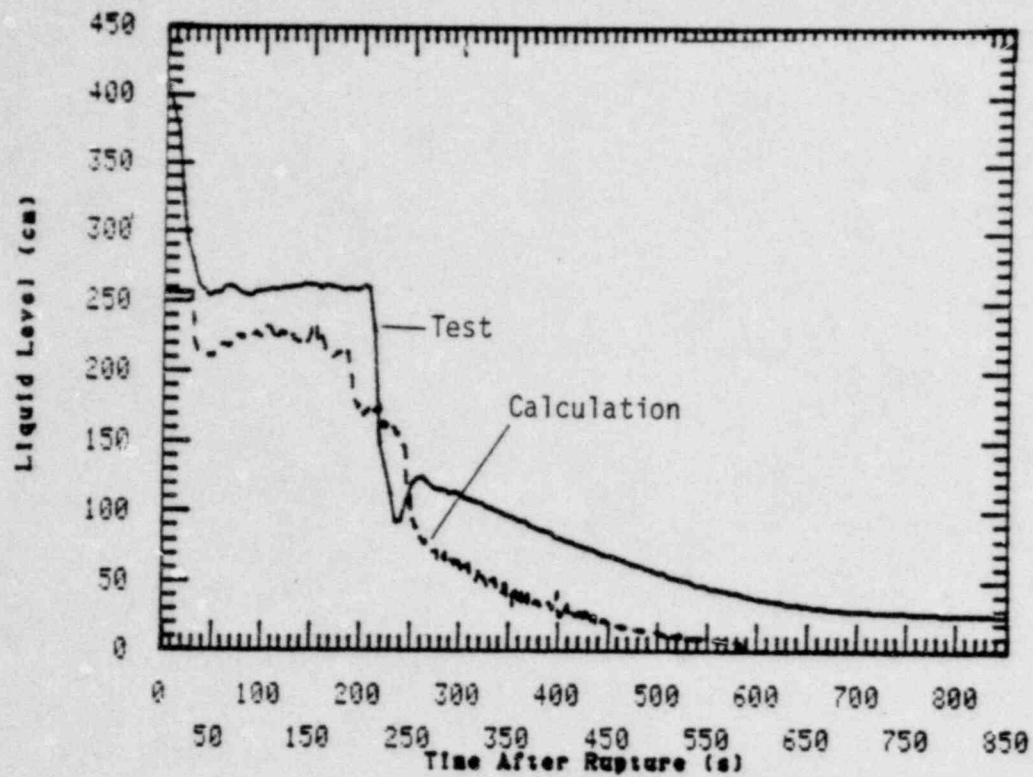


(a)

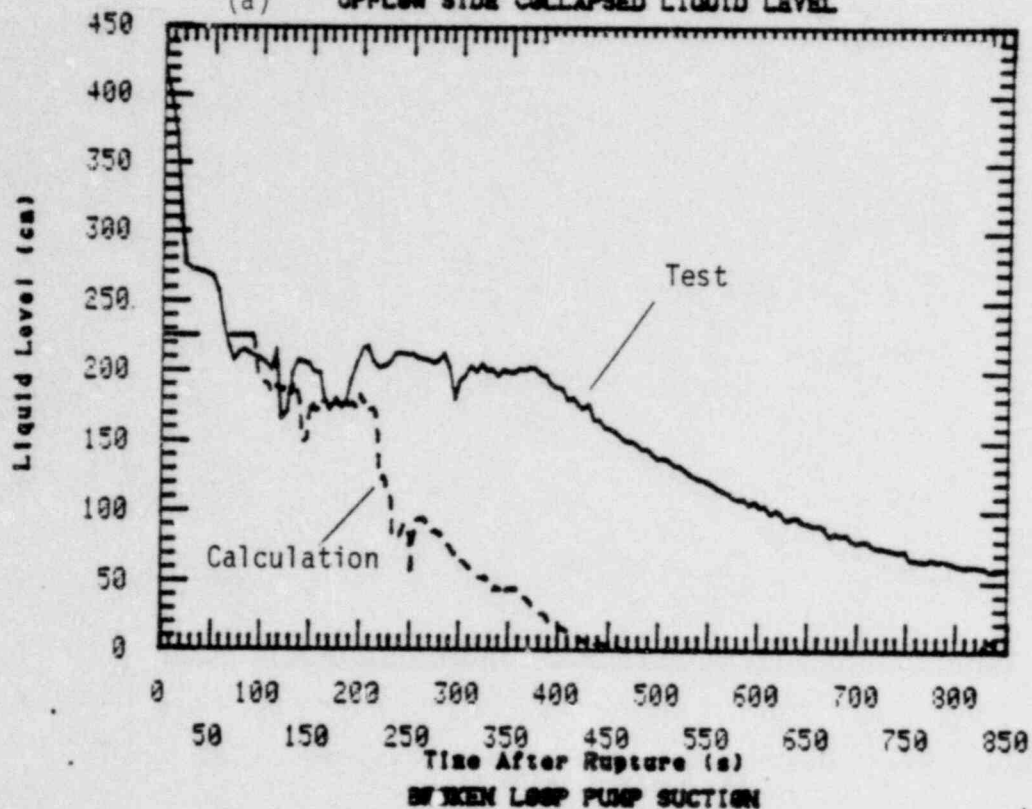


(b)

Figure 37. Comparison of the calculated and measured pump suction liquid levels (downflow side) for Test S-UT-6.



(a) UPFLOW SIDE COLLAPSED LIQUID LEVEL



(b) UPFLOW SIDE COLLAPSED LIQUID LEVEL

Figure 38. Comparison of the calculated and measured pump suction levels (upflow side) for Test S-UT-6.

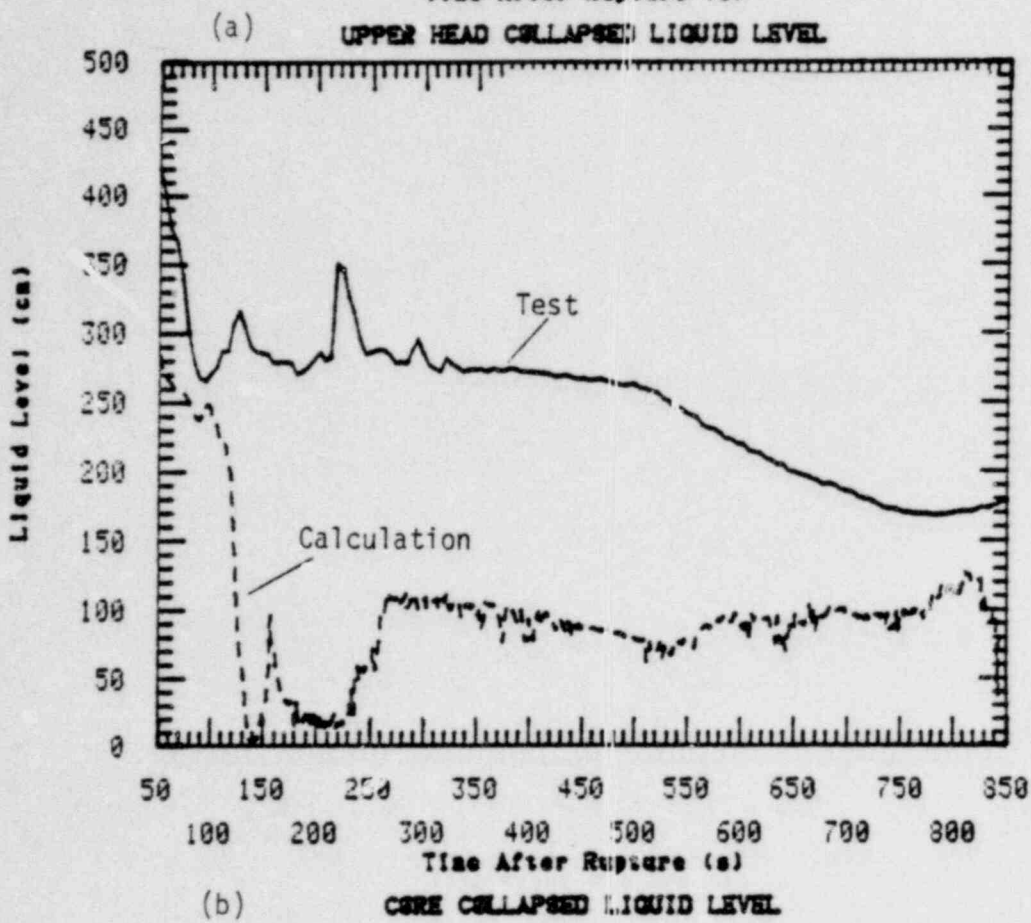
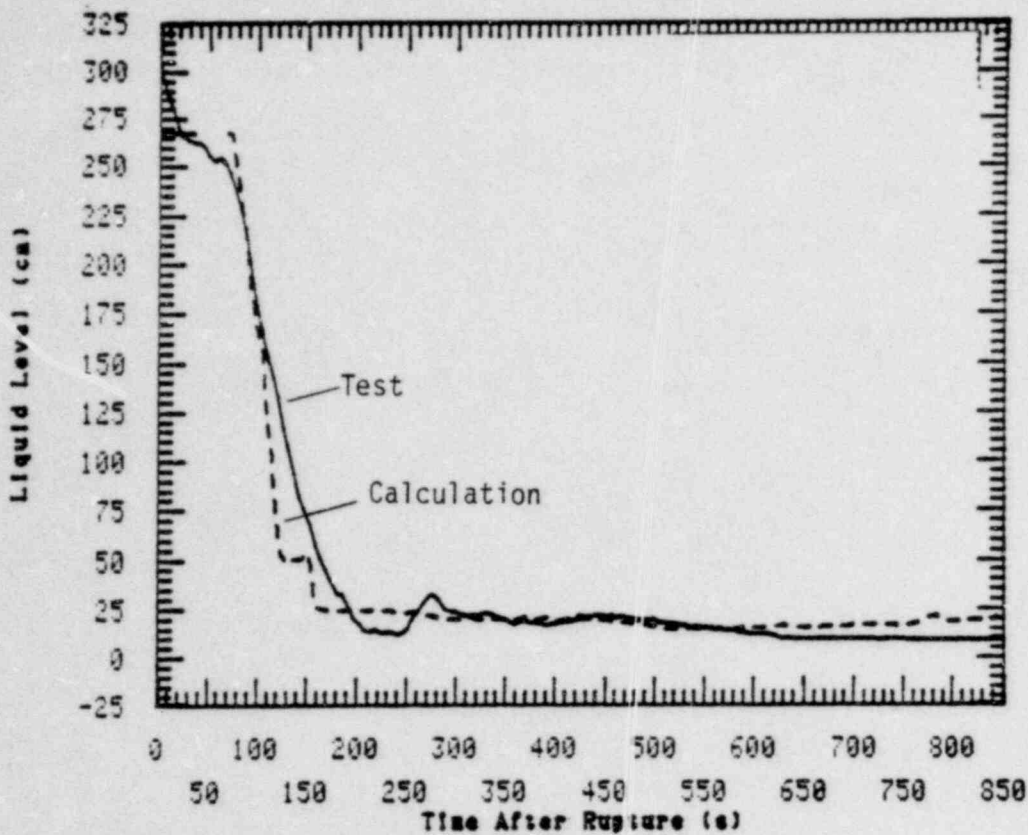


Figure 39. Comparison of calculated and measured upper head and core collapsed liquid levels for Test S-UT-6.

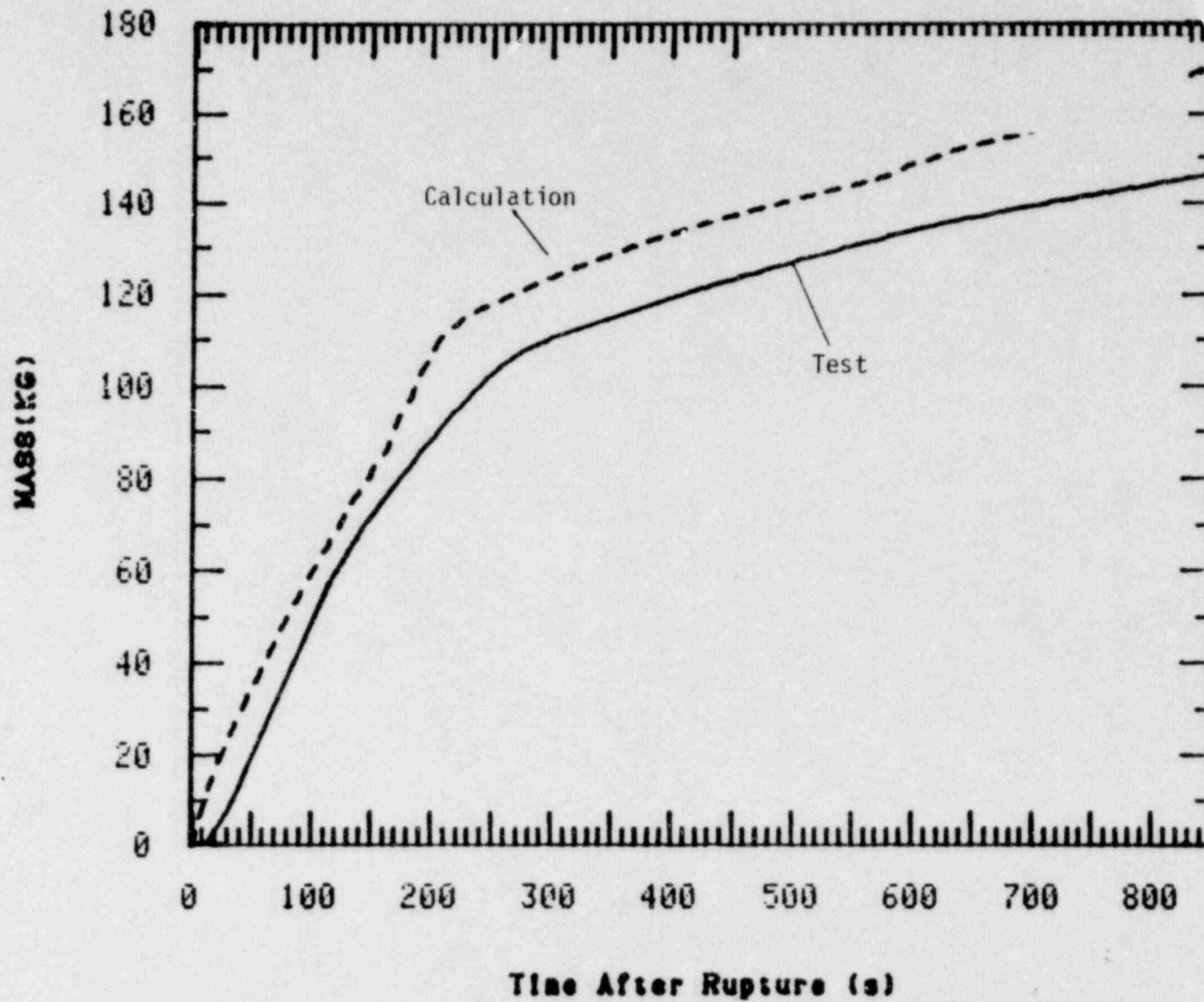


Figure 40. Comparison of the calculated and measured integrated break mass flow rates for Test S-UT-6.

The second reason for underpredicting vessel coolant level is the calculation of a core flow reversal during the period 100 to 200 s which does not occur in the test. In addition, reverse flow oscillations in the lower core were calculated to occur continuously after 200 s. The flow reversals prevented HPIS coolant from entering the vessel. This caused almost total core uncover (minimum level of 6 cm) between 130 s and 250 s.

The difference between the measured and calculated core liquid level is reflected in the significantly different heater rod surface temperature responses. The test prediction indicated that heater rod surfaces in the upper 75% of the core would undergo temperature excursions much larger than observed in the test. Figure 41 shows the calculated and measured peak heater rod responses for the core region between 30 and 60 cm below the top of the core. Prolonged core dryout caused the calculated heater rod temperature to reach 680 K whereas the corresponding measured temperature response shows dryout occurring much later and producing a smaller peak heater rod temperature of 660 K. The calculated temperature excursion turns over at 560 s after the intact and broken loop accumulators are activated at 535 s. Likewise, the corresponding measured temperature excursion turns over at 850 s, after the accumulators were activated at approximately 740 s.

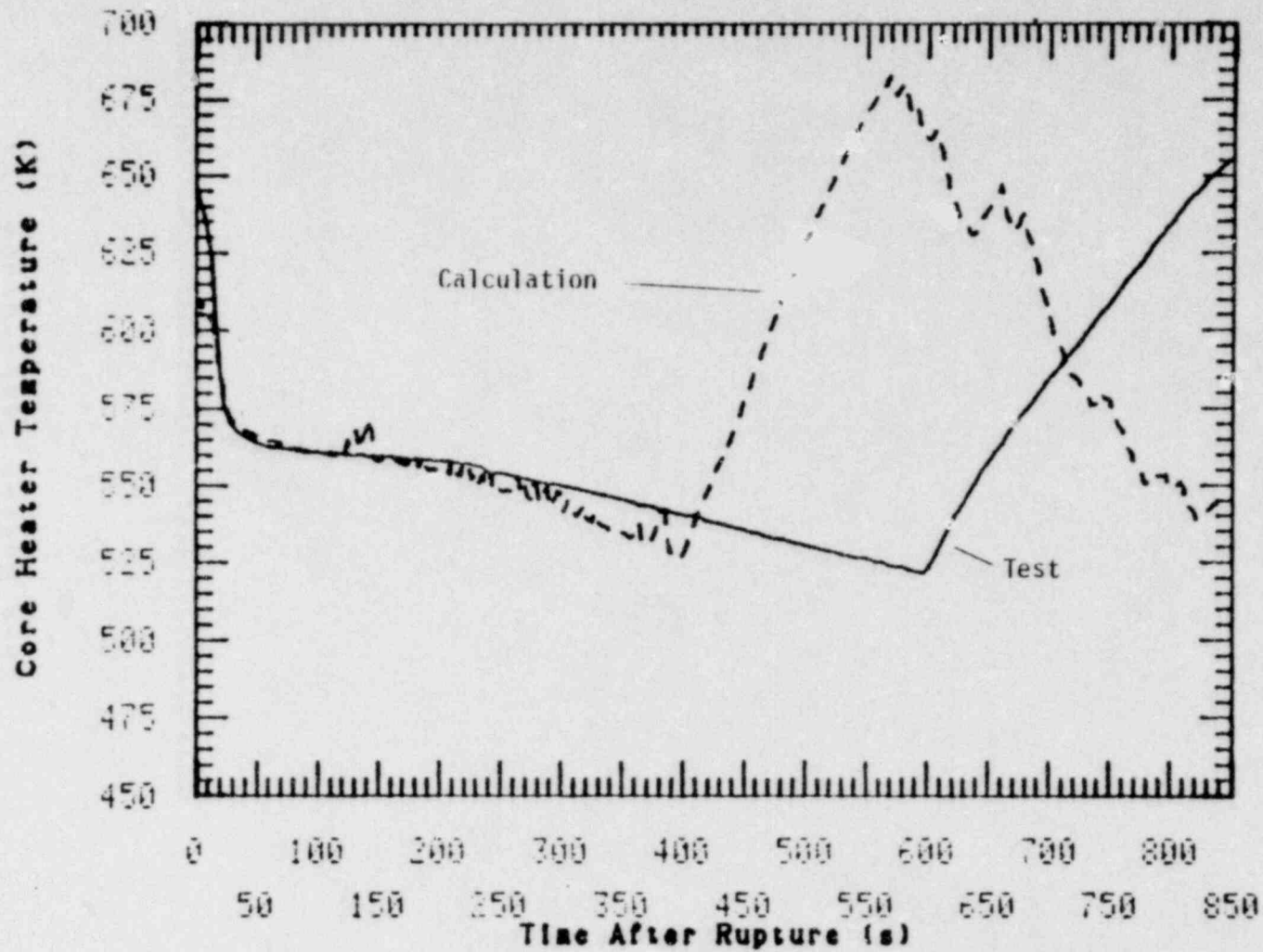


Figure 41. Comparison of calculated and measured core heater rod cladding temperature at the midcore region for Test S-UT-6.

5. CONCLUSIONS

Results from Test S-UT-6 have provided information about system pressure response, break flow, fluid mass distribution, core response and ECC injection effects for a 5% communicative cold leg break loss-of-coolant experiment with cold leg ECC injection. The test met its objective of providing baseline data that are to be used for comparison to Test S-UT-7 (a similar test with upper head injection), as well as meeting the objective of providing the thermal-hydraulic data necessary for assessing computer code performance.

Results from Test S-UT-6 indicate that the break flow rate during the early part of the transient is large enough, relative to the HPIS flow rate, to cause uncovering of the upper part of the core prior to the initiation of accumulator injection. The core uncover is a result of a gradual boiloff of the vessel liquid inventory, rather than a result of level depression due to loop seal formation. The temperature excursion that occurred when the core became uncovered was of limited consequence, since the peak cladding temperatures observed were somewhat less than the cladding temperatures at normal steady-state operating conditions. Once accumulator injection began and through the remainder of the transient, ECC addition to the system was sufficient to cause a gradual increase in the primary system mass inventory, thus ensuring that the core remained covered.

Calculated trends from the RELAP5 test prediction generally compared well with the test data. However, the predicted magnitudes of many of the corresponding trend system parameters were not in good agreement with the test data. Posttest analysis will be required to fully account for these deficiencies in the calculation.

6. REFERENCES

1. T. K. Larson, J. L. Anderson, and D. J. Shimeck, Scaling Criteria and An Assessment of Semiscale Mod-3 Scaling for Small Break Loss-of-Coolant Transients, EGG-SEMI-5121, EG&G Idaho, Inc., March 1980.
2. System Design Description for the Mod-3 Semiscale System (Revision B), EG&G Idaho, Inc., December 1980.
3. P. North letter to R. E. Tiller, Experiment Operating Specification for Semiscale Mod-2A 5% Break Experiment, Tests S-UT-6 and S-UT-7, PN-38-81, EG&G Idaho, Inc., April 8, 1981.
4. P. North letter to R. E. Tiller, Test Prediction for Semiscale Mod-2A Small Break Test S-UT-6, PN-40-81, April 16, 1981.

APPENDIX A

APPENDIX A

The pretest prediction calculation for Semiscale Mod-2A Test S-UT-6 was executed using RELAP5/MOD1 (Version 6) (Idaho National Engineering Laboratory Configuration Control Number F00181). The input deck for the S-UT-6 calculation is stored under the INEL configuration control number F00227. This is an experimental version of the code. The model nodalization diagram used for the calculation is shown in Figure A-1. The model consists of 164 hydrodynamic volumes and 154 heat structures. All volume parameters are calculated with nonequilibrium code models. Break flow multipliers of 0.8 and 0.9 were used for the subcooled and two-phase discharge coefficients respectively.

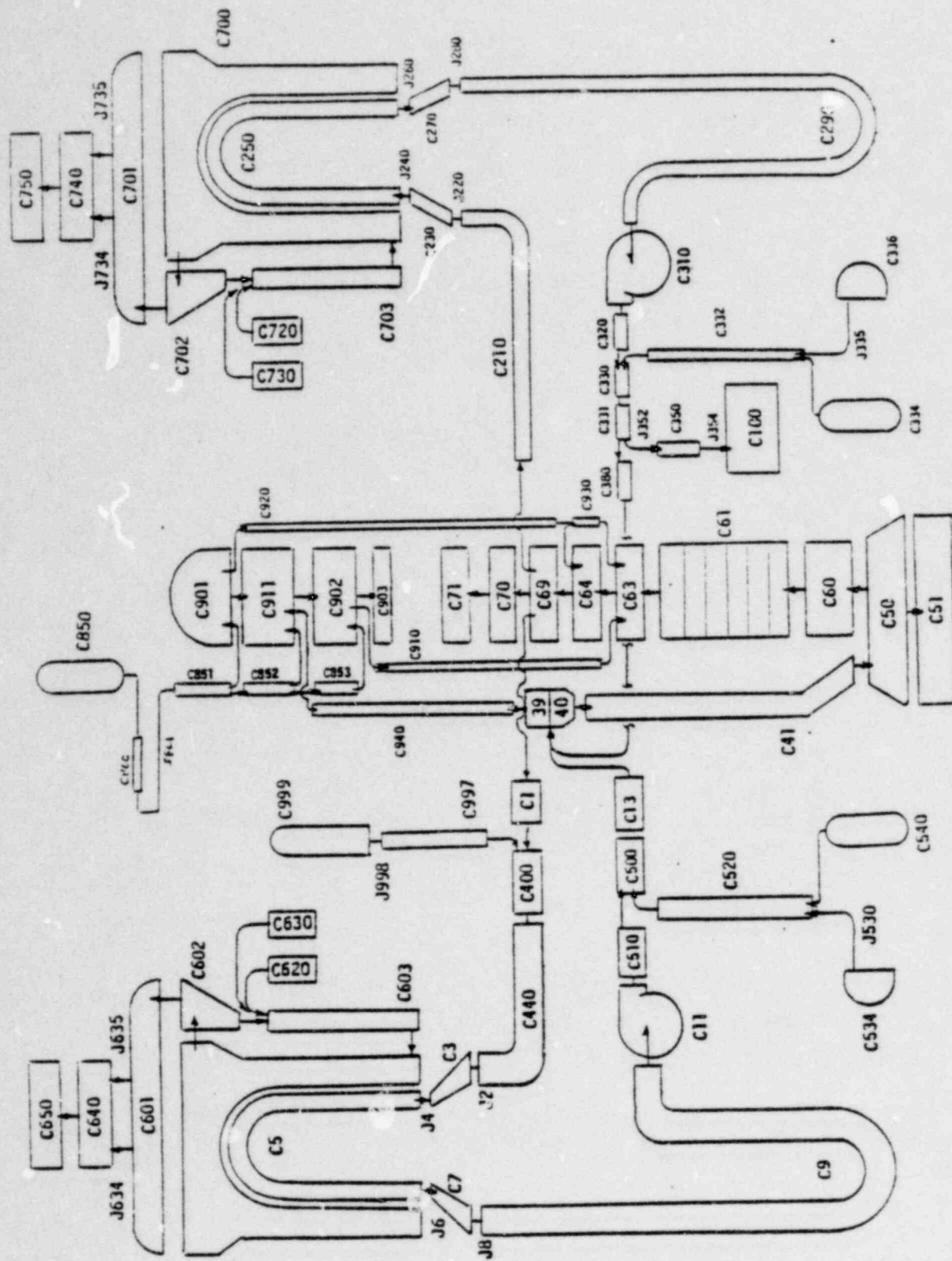


Figure A-1. Nodalization diagram of the RELAP5 model for the Semiscale Mod-2A system.